



Università Campus Bio-Medico di Roma

**Corso di dottorato di ricerca in Scienze Biomediche
Integrate e Bioetica
XXXVIII ciclo a.a. 2022-2023**

**Risk stratification in MASLD patients using non-invasive
approaches: application of electronic multi-sensoring
technologies**

Francesca Terracciani

Director
Prof. Raffaele Antonelli Incalzi

Supervisor
Prof. Umberto Vespasiani Gentilucci

22 April 2026

*To my loved ones, in every form they take.
To my work, and to the passion that lives within it.
To all those who suffer and deserve a chance.*

*Ai miei affetti, in ogni declinazione.
Al mio lavoro, e alla passione che lo abita.
A tutte le persone che soffrono e meritano una possibilità.*

ABSTRACT

Francesca Terracciani

Unit of Clinical Medicine and Hepatology, Fondazione Policlinico Universitario

Campus Bio-medico di Roma, Italy;

Research Unit of Hepatology, Università Campus Bio-medico di Roma, Italy.

Background and aims: Fibrotic MASH, the inflammatory form of MASLD with significant activity and fibrosis (necroinflammatory activity -NAS score- ≥ 4 and fibrosis ≥ 2), and advanced fibrosis (fibrosis stage ≥ 3) represent the most treatment-requiring and prognostically relevant phenotypes of MASLD. For this reason, much research is focusing on identifying non-invasive tools capable of diagnosing this condition. In the last years, multisensory analysis techniques are emerging as diagnostic/prognostic tools potentially useful in various disorders, including liver diseases. This thesis aimed to evaluate the diagnostic performance of these technologies for risk stratification in MASLD, with particular focus on the identification of patients with fibrotic MASH and significant/advanced fibrosis.

Methods: This was a prospective, exploratory feasibility study conducted at the Fondazione Policlinico Universitario Campus Bio-Medico di Roma. Consecutive patients with MASLD or metabolic risk factors were enrolled between December 2022 and December 2025. Two cohorts were defined: a non-invasive cohort, in which fibrotic MASH and fibrosis were assessed using the FAST score and liver stiffness measurement (LSM) by FibroScan®, and a histological cohort, in which disease was characterized by liver biopsy. All participants underwent breath, urine, and saliva sampling, analyzed using the BIONOTE e-nose and e-tongue systems, respectively. Diagnostic performance was evaluated using elastic net-regularized logistic regression with 10-fold stratified cross-validation, and reported as AUC, accuracy, sensitivity, specificity, PPV, and NPV.

Results: A total of 215 patients were included (158 in the non-invasive and 57 in the histological cohort, mean age 56.6 ± 13.9 years; 65% male; median BMI 31.1 kg/m²). In the overall cohort assessed by non-invasive reference standards (FAST score and LSM), all three biological matrices showed limited diagnostic performance for both fibrotic MASH (AUC 0.54–0.60) and significant fibrosis (AUC 0.56–0.63). In the biopsy-proven cohort, the e-nose demonstrated moderate diagnostic accuracy for fibrotic MASH (accuracy 0.74; AUC 0.78) and significant fibrosis (accuracy 0.74; AUC 0.70), with moderate-to-high specificity and positive predictive value (0.87 and 0.89, respectively). E-tongue analyses showed lower and more variable performance across both matrices and outcomes. Within the histological cohort, the e-nose showed higher accuracy and PPV compared with LSM, whereas FAST retained higher sensitivity and negative predictive value (AUC 0.81 at the rule-out threshold), supporting complementary roles in risk stratification. Subsequent substudies, focused on integrated predictive modeling and metabolomic analysis, are ongoing.

Conclusions: Multisensory electronic technologies showed modest-to-moderate performance in MASLD risk stratification, with the e-nose yielding the most promising results. Their non-invasiveness, rapidity, and scalability support the potential role of e-sensing-derived features as novel complementary components of integrated risk stratification strategies, rather than as stand-alone diagnostic tool.

INDEX

1. Introduction.....	5
1.1 Metabolic dysfunction-associated steatotic liver disease	
1.2 Natural history and prognostic determinants: fibrosis stage and fibrotic MASH	
1.3 Screening and risk stratification strategies	
1.4 Invasive and noninvasive assessment of MASLD and MASH	
1.6 Electronic technologies and applications	
2. Aims and pertinent substudies.....	22
2.1 Evaluation of multisensory electronic technologies as noninvasive tools for the detection of fibrotic-MASH and significant or advanced fibrosis in MASLD patients	
2.2 Development of a multisensory electronic technology-based predictive model for risk stratification and identification of fibrotic MASH and significant or advanced fibrosis (<i>still ongoing</i>)	
2.3 Identification of metabolomic signatures associated with multisensory electronic technology-based assessment of fibrotic MASH and severe liver disease (<i>still ongoing</i>)	
3. Conclusion and future perspectives.....	45
References.....	48

1. Introduction

1.1 Metabolic dysfunction-associated steatotic liver disease (MASLD)

Owing to the increasing prevalence of dysmetabolic conditions, MASLD has emerged as a leading cause of chronic liver disease and represents a major and expanding global health burden^{1,2}.

The term MASLD comprises different conditions, including isolated liver steatosis (metabolic dysfunction-associated steatotic liver, MASL), metabolic dysfunction-associated steatohepatitis (MASH), as well as MASH with fibrosis and up to cirrhosis. MASLD is defined as the presence of excess triglyceride storage in the liver in association with at least one cardiometabolic risk factor and no other cause for hepatic steatosis or chronic liver disease³⁻⁵. MASH is characterized by histological features of hepatocellular ballooning and lobular inflammation^{3,6} and represent the progressive form of the disease, leading to cirrhosis, possible hepatocellular carcinoma (HCC), and the need for liver transplantation^{4,7,8}.

Approximately one third of the global adult population is affected by MASLD, making it the leading cause of chronic liver disease¹ (Figure 1). The global prevalence of MASH is estimated to be approximately 5%^{1,2,7}. This prevalence is significantly higher among individuals with central obesity, visceral adiposity, and type 2 diabetes mellitus (T2DM), reaching pooled prevalence estimates ranging from 44% to 66.4%, and accounting for approximately 75% of MASH cases^{2,9,10}. MASLD is also known to affect lean individuals and children with the global pooled prevalence of 11.2% and 13% respectively, in the general population^{11,12}.

Most individuals with MASLD remain asymptomatic for long periods, with a generally slow disease course, whereas only a minority develops progressive liver injury leading to advanced fibrosis, cirrhosis, and hepatocellular carcinoma^{4,13}.

Given its high global prevalence, strong association with increasingly prevalent metabolic risk factors, and highly variable clinical course, MASLD represents a major

and growing global public health burden, underscoring the importance of identifying individuals at risk of disease progression.

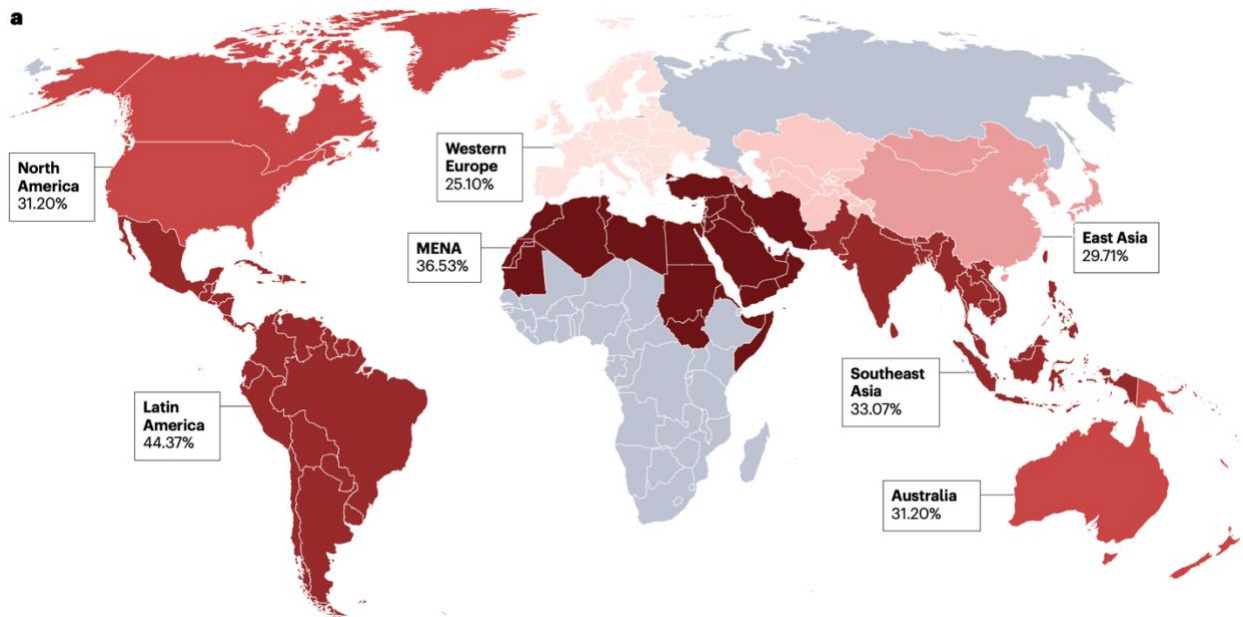


Figure 1. The global prevalence of metabolic dysfunction-associated steatotic liver disease. Data were obtained from a large meta-analysis of 92 studies and the survey included studies from 1990 to 2019 (refs 1,4).

1.2 Natural history and prognostic determinants: fibrosis stage and fibrotic MASH

The pathophysiology of MASLD and MASH involves a complex interplay of metabolic, genetic, and environmental factors². The outdated “two-hit” hypothesis has been replaced by the multiple-hit model, which recognizes genetic predisposition, insulin resistance, adipose tissue dysfunction, gut microbiota alterations, and environmental factors as major contributors to disease progression². Hepatic steatosis represents the central pathogenic event and is driven by excess energy delivery to the liver, adipocyte dysfunction, and systemic insulin resistance, which promote chronic free fatty acid flux and enhanced de novo lipogenesis⁴. In the early stages, hepatic steatosis is characterized by lipid accumulation within hepatocytes in the absence of marked inflammation¹⁴. Development of MASH is caused by excessive lipid deposition into hepatocytes that exceeds the liver’s metabolic capacity². As the disease progresses, oxidative stress, mitochondrial dysfunction, and altered cytokine signalling promote hepatocellular injury and activate inflammatory

pathways¹⁴. These processes facilitate immune cell infiltration and drive the transition from simple steatosis to MASH, which is characterized by hepatocyte ballooning, lobular inflammation, and progressive fibrogenesis, ultimately worsening disease prognosis¹⁴.

The natural history of MASLD is characterized by a generally slow and heterogeneous disease course⁴. Most individuals remain asymptomatic for prolonged periods, and liver-related outcomes affect only a small proportion of patients^{4,13}. The presence of steatosis in the general population is not associated with a clinically meaningful increase in the risk of liver-related outcomes³. MASH represents the progressive form of MASLD and may lead to fibrosis, cirrhosis, hepatic decompensation, and hepatocellular carcinoma^{4,7,8} (Figure 2).

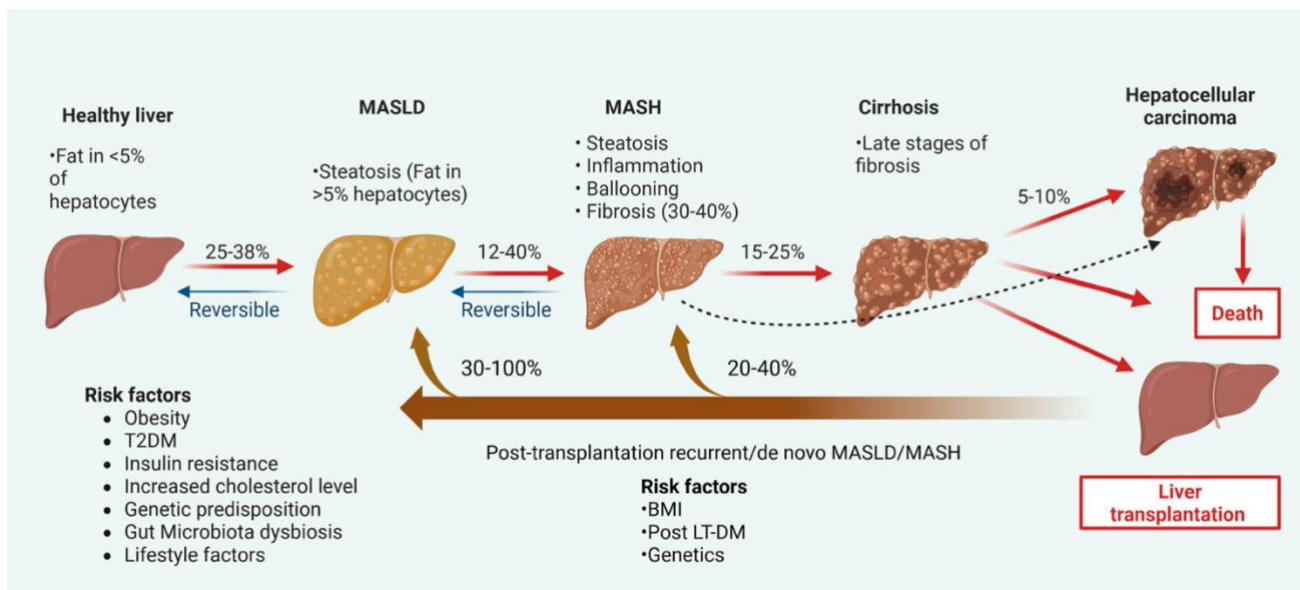


Figure 2. Sequential progression of liver disease and key risk factors (ref 4).

The transition from simple steatosis to steatohepatitis is dynamic, with fibrosis typically progressing more slowly in non-inflammatory MASLD and more rapidly in MASH^{13,15}. However, progression remains heterogeneous, with most individuals showing slow trajectories and a smaller subset, more frequently among patients with

MASH, exhibiting accelerated fibrosis progression, driven by metabolic, clinical, and genetic susceptibility^{13,15}.

Several studies have demonstrated that hepatic fibrosis stage represents the main determinant of long-term outcomes in MASLD, rather than the presence of MASH per se¹⁶⁻²⁰, whereas the NAFLD Activity Score (NAS) and other histological features are more closely associated with short-term disease progression or regression¹⁷.

Although liver fibrosis is the strongest predictor of prognosis in MASLD patients, the propensity of the disease to further progress and the rate at which progression occurs, at any given fibrosis stage, provide equally relevant prognostic information²¹. Indeed, disease activity may follow slow or rapid trajectories²², or even stabilize completely, either spontaneously or in response to therapeutic interventions, potentially leading to fibrosis regression²³ (Figure 3).

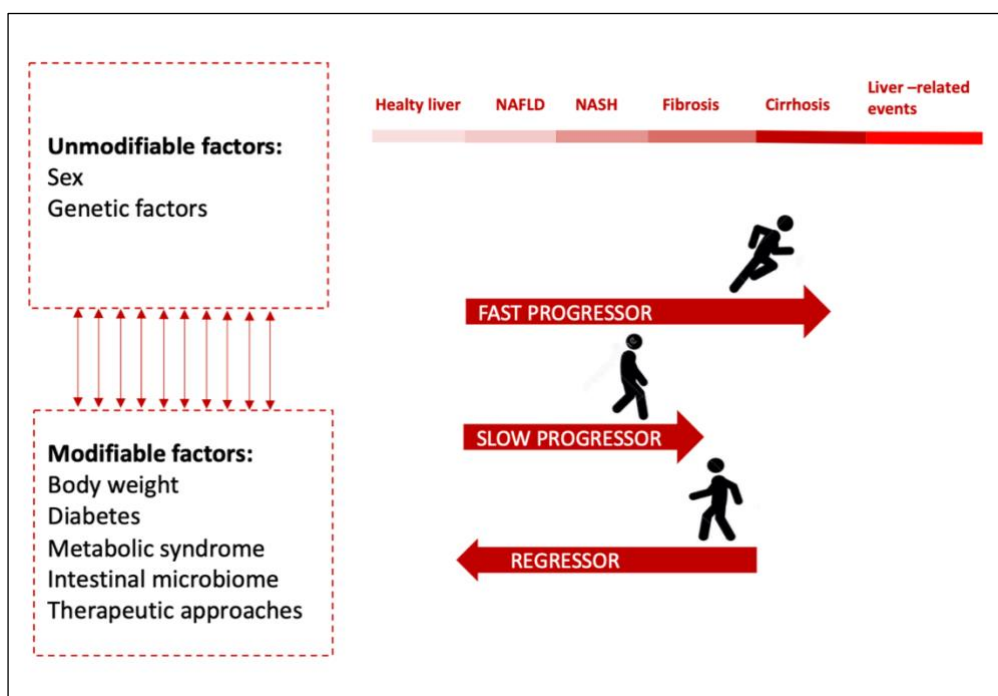


Figure 3. Different trajectories of MASLD, influenced by unmodifiable and modifiable factors (ref 21).

Several factors influence disease progression, including metabolic comorbidities, genetic susceptibility, and environmental exposures. Type 2 diabetes and obesity, particularly central obesity, are the metabolic diseases with the strongest impact on the

natural history of MASLD, including progression to MASLD/MASH-related advanced fibrosis, cirrhosis and hepatocellular carcinoma³. Moreover, individuals with multiple cardiometabolic risk factors are at increased risk of progressive fibrosis and liver-related complications³.

Genome-wide association studies have demonstrated a substantial heritable component in MASLD and MASH and have identified several genetic variants associated with disease susceptibility and progression²⁴. In particular, polymorphisms in genes involved in lipid and glucose metabolism and inflammation, including PNPLA3, TM6SF2, GCKR, MBOAT7, and HSD17B13, have been linked with susceptibility to MASLD and risk of fibrosis progression and liver-related outcomes^{25,26}. The impact of these variants is further modulated by metabolic and environmental factors, highlighting the interaction between genetic predisposition and acquired risk in determining disease trajectories^{14,25,26}.

Altogether, the cumulative burden and interaction of genetic and acquired risk factors determine an individual profile of hepatic steatosis and necroinflammatory and fibrogenic activity, which may remain stable or vary substantially over time²¹. Disease activity and the balance between inflammatory and reparative phases appear to be key determinants of fibrosis remodeling²³.

Fibrotic MASH, characterized by significant inflammatory activity and fibrosis (NAS score ≥ 4 and fibrosis ≥ 2), is recognized as the main driver of progressive liver disease and adverse clinical outcomes^{8,15,17,20,27–29}. Moreover, these individuals are ideal candidates for inclusion in clinical trials investigating novel therapies for MASH and for treatment with newly approved drugs^{29–33}.

In this context, the identification of patients with fibrotic MASH, as well as those with significant/advanced fibrosis, is crucial for optimizing healthcare strategies and resource allocation.

1.3 Screening and risk stratification strategies

While there is no doubt that MASLD is highly prevalent, the absolute risk of liver-related events from MASLD in the general population is very low³.

According to current guidelines, screening for MASLD is not recommended in the general population, while should be offered to individuals at risk, namely those affected by T2DM or obesity with 1 or more cardiometabolic risk factor(s) or with persistent elevation of transaminases^{3,7,34}. A multi-step process is recommended to identify individuals with advanced fibrosis³ (Figure 4). The first step for the identification of high-risk MASLD is calculation of the fibrosis-4 (FIB-4) score. Individuals with FIB-4 scores <1.3 (<2.0 for those ≥65 years old) are considered low risk for advanced fibrosis or adverse outcomes and should continue management in the primary care setting, with consideration for retesting every 1 to 3 years, depending on the presence of risk factors. Individuals with FIB-4 scores ≥1.3 (≥2.0 for those ≥65 years old) should undergo second-line NITs, such as VCTE, to measure liver stiffness. The first-line test should be conducted in primary care or non-gastrointestinal/hepatology settings. Although the second-line test can be conducted in the same settings, VCTE is performed primarily at gastroenterology or hepatology practices⁷.

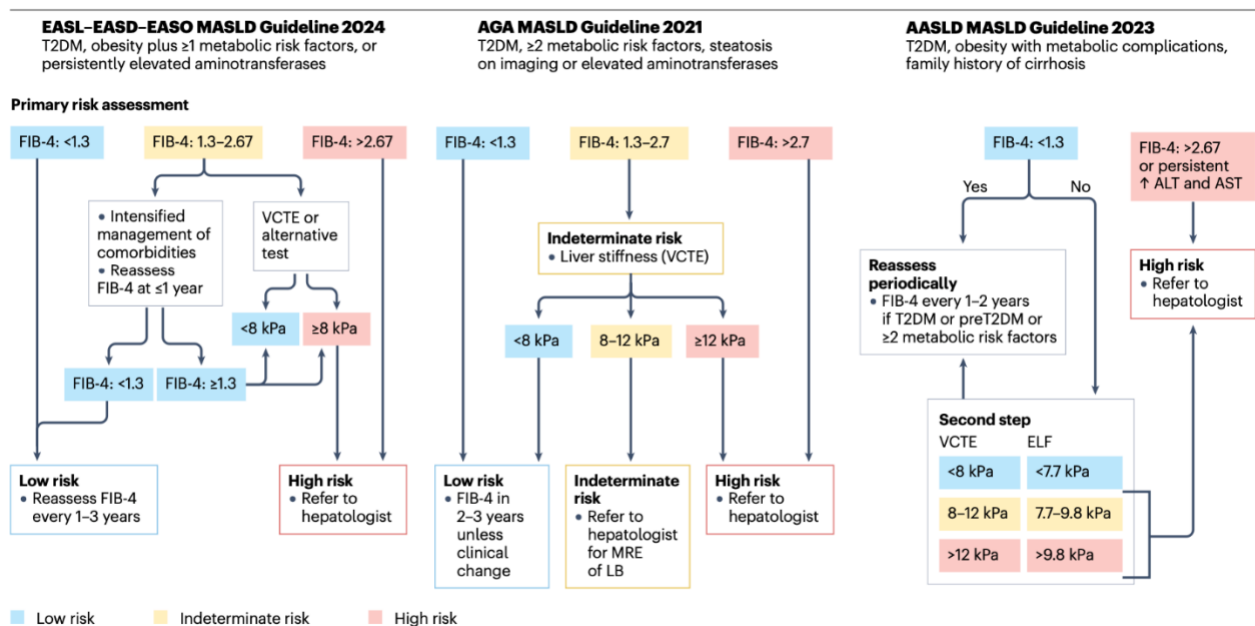


Figure 4. Proposed strategy for non-invasive assessment of the risk for advanced fibrosis and liver-related outcomes in individuals with metabolic risk factors or signs of SLD. ALT, alanine aminotransferase; AST, aspartate aminotransferase; ELF, enhanced liver fibrosis; FIB-4, fibrosis-4 index; MRE, magnetic resonance elastography; SLD, steatotic liver disease; VCTE, vibration-controlled transient elastography; LB, liver biopsy; AASLD, American Association for the Study of Liver Diseases; AGA, American Gastroenterological Association; EASL, European Association for the Study of the Liver; EASD, European Association for the Study of Diabetes; EASO, European Association for the Study of Obesity, (ref 14).

1.4 Invasive and noninvasive assessment of MASLD and MASH

While histological assessment remains the gold standard for the diagnosis of steatosis, fibrosis and MASH, its routine use in clinical practice has declined^{3,4,34}. Liver biopsy is an invasive procedure, associated with potential risks and is limited by high costs, sampling variability, and inter- and intra-observer variability^{35,36}, making it unsuitable for population-level screening and restricting its use to selected individuals. Indeed, current guidelines support a non-invasive, stepwise approach, reserving liver biopsy for cases with diagnostic uncertainty, discordant non-invasive tests, or suspected alternative liver diseases^{3,34}.

In the last decades, the noninvasive assessment of liver fibrosis has been extensively explored, leading to different clinical and biochemical scoring systems and imaging-based approach³⁷.

Blood-based biomarkers tools for advanced fibrosis

Currently, the fibrosis-4 index (FIB-4, non-patented) and the enhanced liver fibrosis test (ELF, patented) are the most widely adopted serum biomarkers. Overall, non-invasive scores are highly effective at ruling out advanced fibrosis, showing high negative predictive values (NPVs >90%). However, their positive predictive values (PPVs) are often modest, and they are unable to accurately discriminate the different fibrosis stages³⁸.

The best diagnostic accuracy, especially with respect to ruling-out advanced fibrosis, was displayed by FIB-4 and NAFLD fibrosis score (NFS). The FIB-4 score (age, AST, ALT, platelet count) was found to be one of the best performing, with an AUROC of

0.86 for advanced fibrosis (0.78–0.94)³⁹. Values <1.3 effectively rule out advanced fibrosis in NAFLD, while those >2.67 identify individuals with advanced fibrosis. In clinical practice, the lower (high sensitivity) threshold is the most used given that the NPV is most robust³⁸. In addition to FIB-4, the NFS (age, type 2 diabetes, BMI, AST/ALT, albumin, platelet count) was found to be the other best-performing simple biomarker for advanced fibrosis. NFS was developed in an international cohort of individuals with biopsy-proven NAFLD with an area under the receiver operating characteristic (AUROC) of 0.81 (0.71–0.91)⁴⁰. Values <-1.455 exclude advanced fibrosis with high accuracy and values >0.676 diagnose advanced fibrosis with improved PPV. This score has been independently validated in several studies³⁸.

Enhanced liver fibrosis (ELF), Fibrometer and Fibrotest are biochemical algorithms with higher sensitivities and specificities and better AUROC for identifying patients with advanced fibrosis, but they are proprietary tests and, as such, more expensive and less available in the ordinary clinical practice²¹.

The ELF test is a panel of direct markers of fibrosis and matrix turnover, namely hyaluronic acid, pro-collagen III (PRO-C3), and tissue inhibitor of metalloproteinase 1 (TIMP1). It was first developed in individuals with HCV, and subsequently validated in MASLD with an AUROC of 0.90 (0.84-0.96)⁴¹. In MASLD, the ELF threshold <7.7 (low threshold recommended by the manufacturer) demonstrated high sensitivity of 0.93 (0.82-0.98) but low specificity of 0.34 (0.13-0.65), whereas the ELF threshold >9.8 (high threshold recommended by the manufacturer) showed a specificity of 0.86 (0.77-0.92) and sensitivity of 0.65 (0.49-0.77). Importantly, the NPV was good when the prevalence of advanced fibrosis ranged from 5-10%, while the PPV was less strong⁴².

Regarding the capability of predict clinical outcomes, most studies identified FIB-4 and NFS as the scores with the higher prognostic potential and accuracy in predicting overall mortality and liver-related events. Interestingly, some studies suggest that repeated assessments of the scores over time can improve their predictive power.

Imaging-based tools for advanced fibrosis

Beyond serum-based scores, non-invasive assessment of liver fibrosis also relies on physical approaches based on the measurement of liver stiffness. The underlying assumption is that increasing tissue stiffness reflects progressive extracellular matrix deposition and fibrosis. Liver stiffness can be quantified using different imaging-based techniques. Among these, vibration-controlled transient elastography (VCTE) is supported by the largest body of evidence. Using the FibroScan® device, VCTE measures the velocity of low-frequency shear waves propagating through the liver. The same platform also enables assessment of hepatic steatosis through the controlled attenuation parameter (CAP)^{21,37}. Large validation studies have demonstrated that VCTE provides good to excellent accuracy for detecting clinically significant and advanced fibrosis in MASLD, supporting its role in non-invasive risk stratification^{43,44}. Notably, subcutaneous adipose tissue and fluid may attenuate elastic waves, limiting feasibility and reliability in patients with obesity or ascites³⁷. This limitation has been partially addressed by the introduction of the extra-large (XL) probe, specifically designed for individuals with increased body mass. Although liver stiffness thresholds may vary across etiologies, a cut-off below 8 kPa appears appropriate to reliably exclude advanced fibrosis in routine clinical practice^{35,45}. Point shear-wave elastography (pSWE) based on acoustic radiation force impulse (ARFI) technology measures tissue displacement induced by short-duration, high-intensity acoustic pulses. Its main advantages include real-time anatomical visualization, applicability in the presence of ascites, and direct integration into conventional ultrasound systems³⁷. Magnetic resonance elastography (MRE) is an MRI-based technique that quantifies liver stiffness using dedicated hardware and software⁴⁶. Among non-invasive modalities, MRE shows the highest diagnostic accuracy for fibrosis staging in MASLD, including early disease stages^{46,47}. A detailed meta-analysis has confirmed these performance characteristics with AUROCs of 0.91 (sensitivity 78%, specificity 89%) for significant fibrosis \geq F2, 0.92 (sensitivity 83%, specificity 89%) for advanced

fibrosis \geq F3 and 0.90 (sensitivity 81%, specificity 90%) for cirrhosis in MASLD⁴⁸. Nevertheless, high costs and limited availability currently restrict its use primarily to tertiary centers and research settings. Moreover, pSWE/ARFI and two-dimensional shear-wave elastography are not currently included in major clinical guidelines owing to the limited amount of data²⁹.

Two new transient elastography-based scores, Agile 4 and Agile 3+ (LSM, AST/ALT ratio, platelet counts, age, sex, diabetes status), were recently developed to identify cirrhosis and advanced fibrosis, respectively, in individuals with NAFLD in secondary/tertiary care liver clinics. Substantially, both Agile 4 and Agile 3+ showed a higher performance than FIB-4 and LSM for cirrhosis or advanced fibrosis, with an AUROC of 0.91 (0.89-0.92) and 0.90 (0.88-0.91), respectively, in the training cohorts⁴⁹.

Noninvasive tools for identifying individuals at risk of fibrotic MASH

Given the major prognostic impact of fibrotic MASH, considerable efforts over recent decades have focused on developing non-invasive tools capable of identifying this high-risk condition. Several composite scores integrating serum and imaging biomarkers have been proposed, showing variable diagnostic performance and predictive values.

Blood based biomarkers comprise MACK3, Fibrotic NASH Index (FNI), NIS4 and NIS2+, and omics models, such as NASH ClinLipMet and the Metabolomics-Advanced StEatohepatitis Fibrosis (MASEF) score. Imaging-based biomarkers include magnetic resonance imaging (MRI)-derived iron-corrected T1, whereas combined approaches integrating imaging and blood biomarkers comprise the FibroScan-AST (FAST) score, the magnetic resonance imaging–AST (MAST) score, and the MEFIB index. Table 1 summarizes diagnostic performance metrics (AUROC, sensitivity, specificity, PPV, and NPV), as well as the main strengths and limitations, of validated composite scores for fibrotic MASH.

Score	Components	Target	AUROC	Rule-out Sensitivity,%	Rule-out Specificity,%	NPV	Rule-in Sensitivity,%	Rule-in Specificity,%	PPV	Main Strengths	Main Limitations	Key References
FAST	VCTE (LSM + CAP) + AST	At-risk MASH / $\geq F2$	0.85 (0.83-0.87)	89	64	0.94 (0.73–1.00)	49	92	0.69 (0.33–0.81)	Widely available, automated	Grey zone, expensive for primary care	Newsome et al. Lancet 2020; Ravaoli et al. Gut 2023
MEFIB	MRE + FIB-4	$\geq F2$ / At-risk MASH	0.768 (0.728–0.808)	91.5	56.2	0.94	59.9	77.7	0.55	Best head-to-head performance	Limited MRE availability	Jung et al. Gut 2021; Kim et al. J Hepatol 2022
MAST	MRI-PDFF + AST	At-risk MASH	0.93 (0.88–0.97)	89	72	98	75	90	0.50	Excellent rule-out performance	MRI access	Noureddin et al. J Hepatol 2022
MACK-3	HOMA-IR + AST + CK-18	Fibrotic MASH / $\geq F2$	0.79 (0.77–0.81)	90	48	0.85–0.95	48	86	0.25–0.85	Strong biological rationale	CK-18 not routine	Boursier et al. Hepatology 2018; Canivet et al. CGH 2023
NIS2+	miR-34a + YKL-40	At-risk MASH	0.813 (0.795–0.832)	85	61	0.83	62	85	0.77	Stable across metabolic subgroups	Trial-based validation	Harrison et al. J Hepatol 2023
FNI	HDL + AST + HbA1c	Fibrotic MASH	0.80–0.95	87–100	22–54	0.99–1	34–82	73–98	0.12–0.49	Simple blood-based score	Limited external validation	Tavaglione et al. CGH 2023

Table 1. Characteristics and performance metrics of composite scores for fibrotic MASH

MACK-3, a blood test combining aspartate transaminase, homeostasis model assessment of insulin resistance and cytokeratin-18, was validated in a multicentric cohort of 1,924 biopsy-proven patients with MASLD, achieving an AUROC of 0.79 for fibrotic MASH and a diagnostic accuracy comparable to that of FAST^{50,51}. Despite its strong biological rationale linking metabolic dysfunction and hepatocellular injury, MACK-3 is not currently endorsed by clinical guidelines and requires biomarkers, such as cytokeratin-18, that are not routinely available in clinical practice.

The FNI, derived from an Italian cohort of biopsy-confirmed patients, integrates high-density lipoprotein, AST, and HbA1c. Its diagnostic performance was satisfactory in both derivation and external validation cohorts, with AUROCs ranging from 0.78 to 0.95 and high negative predictive values for rule-out⁵². Its main advantage lies in the exclusive use of routinely available laboratory parameters, supporting broad applicability, although its performance may be influenced by metabolic comorbidities and disease prevalence.

Similarly, NIS4®, a blood-based panel including $\alpha 2$ -macroglobulin, HbA1c, YKL-40, and miR-34a, demonstrated good accuracy for detecting at-risk MASH, with an AUROC of 0.80⁵³. Its optimized successor, NIS2+™, combining miR-34a-5p and YKL-40, showed improved performance across relevant clinical subgroups. However,

available validation data are largely derived from trial-based populations, and broader real-world validation remains warranted⁵⁴.

Among omics-based approaches, NASH ClinLipMet integrates clinical, genetic, lipidomic, and metabolomic data and identifies NASH with an AUROC of up to 0.88⁵⁵. The MASEF score utilizes lipids, ALT, AST, and BMI to evaluate MASH, achieved moderate accuracy in validation cohorts with validation cohorts showing an AUROC of 0.79⁵⁶. Nevertheless, the complexity, cost, and limited accessibility of omics platforms currently restrict their routine clinical application.

Among imaging-based biomarkers, MRI-derived iron-corrected T1 (cT1) has been validated for distinguishing at-risk MASH with an AUROC of 0.78 in biopsy-confirmed MASLD patients. Combining cT1 with MRI-derived steatosis metrics slightly improved performance (AUROC 0.79)⁵⁷. Its non-invasive assessment of fibroinflammatory activity represents a major advantage; however, limited availability, cost, and lack of widespread standardization currently hamper large-scale adoption.

Combining imaging and circulating biomarkers has yielded superior diagnostic performance for at-risk MASH². The FAST is a continuous and composite score, combining CAP, LSM by VCTE, and AST level⁵⁸. FAST demonstrated good discrimination in derivation and validation cohorts and has been supported by recent meta-analyses, particularly for rule-out strategies using dual cut-offs⁵⁸⁻⁶⁰. Its main strengths include automated calculation and wide availability through Fibroscan® devices, although its positive predictive value remains moderate and dependent on disease prevalence. Moreover, it is not available in primary care.

The magnetic resonance imaging (MRI)-AST (MAST) score, combining MRI-PDFF, MRE, and AST, showed excellent diagnostic accuracy, outperforming FAST in selected cohorts. Compared to FAST, MAST exhibited a higher AUC and overall better discrimination⁶¹.

Similarly, the MEFIB index, combining MRE and FIB-4, demonstrated high negative predictive value for excluding at-risk NASH, although its primary target remains the detection of significant fibrosis⁶².

These scores are particularly valuable for rule-in strategies and clinical trial enrichment, but their reliance on advanced MRI techniques limits their applicability to specialized centers.

Compared with other composite scores, FAST has been increasingly used in clinical and research settings owing to its simplicity, broad external validation, and feasibility, as it is based on widely available Fibroscan® measurements and routine laboratory parameters. It is inexpensive, rapid, and easily applicable at the bedside, without the need for advanced imaging, and has shown good diagnostic performance, particularly for ruling out fibrotic MASH. However, current clinical practice guidelines do not explicitly recommend FAST as part of the routine diagnostic algorithm.

Despite their overall promising performance, many of these models rely on advanced biomarkers or imaging techniques that are costly, time-consuming, and restricted to specialized centers. These limitations, together with residual indeterminate zones and variable performance across populations, underscore the need for scalable and widely accessible alternatives for the identification of fibrotic MASH².

1.5 Electronic-technologies and application

Under physiological conditions, metabolic processes continuously generate a wide range of metabolites and biochemical by-products. Pathological states are associated with qualitative and quantitative changes in circulating and excreted metabolites, which can be detected in biological matrices and may serve as indirect biomarkers of disease-related processes⁶³. Accordingly, several qualitative and quantitative analytical techniques, including gas chromatography–mass spectrometry (GC-MS), have been developed to characterize metabolic signatures but remain limited in clinical practice by high costs, technical complexity, and long processing times⁶⁴.

In recent years, electronic sensing technologies, including the electronic nose (e-nose) and electronic tongue (e-tongue), have emerged as useful non-invasive tools applicable to a wide range of pathological conditions. These systems, inspired by human olfactory and gustatory systems, are based on devices that mimic human senses and rely on broadly responsive, cross-reactive sensor arrays for gases or liquids^{63,65}. Multisensory platforms, such as the BIONOTE system, further integrate the simultaneous analysis of gaseous and liquid phases from the same biological sample⁶⁶. Although they are not able to identify specific metabolites in the analyzed samples, they are designed to recognize global chemical signatures and can describe characteristic patterns, or “fingerprints”, associated with specific pathological conditions^{63,65}.

Both e-nose and e-tongue systems share a common modular architecture consisting of three main components: (1) a sampling unit, responsible for collecting gaseous or liquid samples; (2) a cross-reactive sensor array, composed of chemical and electrochemical sensors, as well as gravimetric and optical sensing elements; and (3) a signal processing and pattern recognition module⁶³. In e-nose systems, sensors are mainly based on gravimetric, electrical, and optical transduction principles, whereas e-tongue devices predominantly rely on chemical, electrochemical sensors, including potentiometric, amperometric, conductimetric, and membrane-based electrodes. It consists of arrays of electrochemical and chemical sensors, including potentiometric, amperometric, conductimetric, and membrane-based sensors for liquid-phase analysis. The sensor array interacts with analytes, generating electrical, optical, or gravimetric signals that are acquired through dedicated electronic interfaces. These signals are subsequently pre-processed, subjected to feature extraction, and analyzed using multivariate statistical methods and machine learning algorithms^{63,65}. Figure 5 and Figure 6 schematically illustrate the translation of human olfactory and gustatory perception into electronic nose and electronic tongue technologies.

The electronic nose is specifically designed for the detection of volatile organic compounds (VOCs) in exhaled breath and other gaseous samples. Upon exposure to

VOCs, interactions between analytes and sensing materials induce changes in conductivity, potential, or resonance frequency which are converted into digital signals and processed to generate characteristic “breath prints”^{63,67}.

In medical applications, e-nose systems have demonstrated increasing potential for the non-invasive diagnosis and monitoring of oncological, infectious, neurological, and metabolic disorders, including lung cancer, respiratory infections, Parkinson’s disease, Alzheimer’s disease, diabetes mellitus, and metabolic-associated steatohepatitis. These applications are based on the identification of disease-specific VOC profiles reflecting altered metabolic pathways⁶³.

Similarly, the electronic tongue is designed for the analysis of liquid samples, such as saliva, urine, serum, and other biological fluids. Upon interaction with liquid analytes, e-tongue sensors undergo measurable electrochemical variations, which are converted into digital signals and processed to generate characteristic “taste prints”^{65,68}.

Although the electronic nose and the electronic tongue are based on different sensing mechanisms and analyze different biological matrices, they share a common biomimetic approach based on arrays of partially selective sensors and multivariate pattern recognition and can be integrated within a multisensory analytical framework^{66–68}.

The BIONOTE (BIOsensor-based multisensorial system for mimicking Nose, Tongue and Eyes) system represents a notable example inspired by the concept of sensory synesthesia. BIONOTE enables the simultaneous analysis of gaseous, liquid, and optical properties of biological samples using the same biologically derived sensing material, generating a multimodal chemical signature⁶⁶. The core of the BIONOTE system relies on the use of anthocyanins as sensing interfaces. These natural flavonoid pigments exhibit pH sensitivity, metal-binding capacity, strong optical absorption, and metal-ion binding properties, making them highly adaptable for multisensory detection. The system integrates quartz crystal microbalance sensors for VOC

detection and voltammetric electrodes for liquid-phase analysis, combined with dedicated software for data acquisition and feature extraction. The BIONOTE e-nose is based on an array of seven quartz microbalances oscillating at a resonance frequency of 20 MHz and coated with seven different anthocyanins extracted from three different plant tissues: red rose, red cabbage, blue hortensia⁶⁶. After desorption from the adsorbing cartridge, VOCs bind to the sensing layers, inducing a frequency shift that is registered as the sensor response. The sensors are not selective for volatile organic compounds, whose chemical structures remain unknown. The final breath fingerprint consists of 28 responses, derived from the output of 7 sensors operating at four different temperatures (50-100-150-200°C).

The BIONOTE e-tongue uses a liquid sensor array consisting of three electrodes: a working electrode (WE), reference electrode (RE), and counter electrode (CE). A potential excitation signal ranging is applied between the WE and the RE and resulting current is digitally acquired⁶⁹. The input signal is a triangular function ranging from -1 to +1 V, resulting in 500 input voltages. The output signal consists of the corresponding 500 current values measured at the working electrode ⁶⁶. The electrode array consists of silver, platinum, and gold electrodes.

Given the central role of the liver in systemic metabolism, chronic liver diseases are likely to induce qualitative and quantitative alterations in metabolic by-products, which are subsequently eliminated through gases and bodily fluids.

Overall, electronic sensing technologies and integrated multisensory systems offer significant advantages, including non-invasiveness, rapid analysis, low operational costs, and compatibility with real-time monitoring. These features make them attractive tools for large-scale screening, disease monitoring, and risk stratification. Despite current limitations related to standardization and metabolite specificity, their ability to capture complex metabolic patterns highlights their potential role as complementary diagnostic and prognostic instruments.

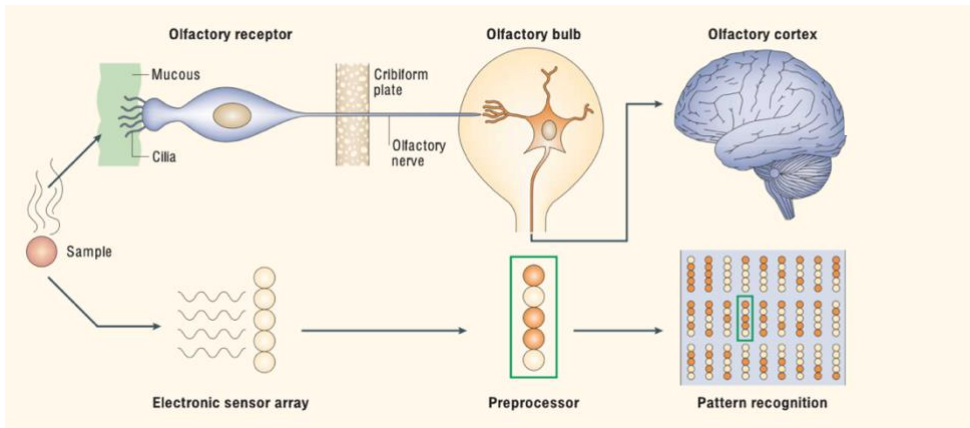


Figure 5. Schematic representation of human olfactory perception and its biomimetic translation into electronic nose systems.

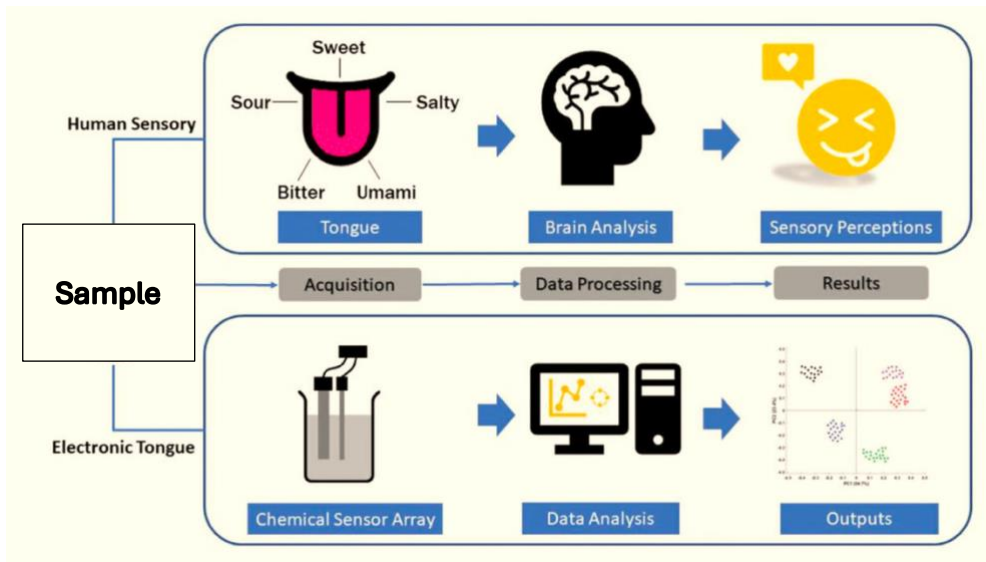


Figure 6. Schematic representation of human taste perception and its biomimetic translation into electronic tongue systems.

2. Aims and pertinent substudies

Fibrotic MASH, along with advanced fibrosis, represents the most clinically relevant phenotype of MASLD and the main target of emerging disease-modifying therapies. Current non-invasive strategies for its identification rely largely on indirect markers of liver injury and fibrosis or on advanced imaging techniques, which, despite good diagnostic performance, remain costly, operator-dependent, and difficult to implement at the population level.

Recent advances in multisensory technologies, such as electronic nose and electronic tongue systems, offer the opportunity to capture complex metabolic signatures through rapid, non-invasive, and scalable approaches.

Against this background, the overall aim of this research is to investigate the potential role of e-sensing technologies as novel non-invasive biomarkers for risk stratification in MASLD and for the identification of high-risk and treatment-eligible patients. Specifically, the aims of this PhD thesis project are:

- 1)** to evaluate the diagnostic performance of e-sensing technologies in identifying patients at high risk of fibrotic MASH or significant/advanced fibrosis;
- 2)** to develop and validate predictive models integrating e-sensing-derived data for individualized risk stratification and the prediction of fibrotic MASH and significant or advanced fibrosis;
- 3)** to characterize metabolomic signatures associated with fibrotic MASH as detected by e-sensing technologies and to investigate their relationship with clinically relevant liver-related outcomes.

2.1

Evaluation of multisensory electronic technologies as noninvasive tools for the detection of fibrotic-MASH and significant/advanced fibrosis in MASLD patients

Introduction

This substudy aims to evaluate the performance of electronic multi-sensing technologies, including electronic nose and electronic tongue, as novel non-invasive tools for stratifying MASLD patients according to their risk of fibrotic MASH and significant/advanced fibrosis.

Specifically, we aim to identify molecular clusters associated with fibrotic MASH or significant fibrosis in a large MASLD cohort, in which fibrotic MASH is defined according to the FAST score and fibrosis stage according to liver stiffness measurement (LSM) by FibroScan®. This approach was adopted to enable testing in a large, real-world population, in which histological assessment is rarely available. The use of validated non-invasive surrogate markers represents a practical and necessary strategy to ensure adequate sample size and statistical power.

To further strengthen the robustness of our findings, we additionally performed analyses in a biopsy-proven subgroup, in which MASH and fibrosis stage were defined according to histological criteria, representing the reference standard. This dual approach allowed us to evaluate the performance of the tools across different clinical settings and reference standards.

Materials and methods

Study design and population

This was a single-center, prospective, exploratory feasibility study, conducted at the Fondazione Policlinico Universitario di Roma (Rome, Italy).

In accordance with the study objectives, consecutive patients diagnosed with MASLD or presenting metabolic risk factors (overweight [BMI ≥ 28 kg/m²], type 2 diabetes mellitus, metabolic syndrome) were recruited from the outpatient hepatology clinics of

the “Fondazione Policlinico Universitario Campus Bio-Medico” between December 2022 and December 2025. Patients with a history of alcohol abuse, viral hepatitis, other causes of chronic liver disease, and/or the use of medications with steatogenic potential were excluded.

Clinical, anthropometric, and biochemical data were collected for all patients. The indication for liver biopsy was determined according to routine clinical practice.

The presence and degree of hepatic steatosis and fibrosis were assessed using the controlled attenuation parameter (CAP) and liver stiffness measurement (LSM), respectively, obtained with the FibroScan® device, or by histological evaluation in patients undergoing liver biopsy.

Fibrotic MASH was defined as a FAST score ≥ 0.67 in patients without histological data⁵⁸ and as histologically confirmed MASH with a NAFLD Activity Score (NAS) ≥ 4 and fibrosis stage ≥ 2 in those with histological assessment⁶. The FAST score was selected as a non-invasive reference standard because of its validated accuracy and its use in clinical practice. Significant fibrosis was defined as a histological fibrosis stage ≥ 2 , whereas advanced fibrosis was defined as a histological fibrosis stage ≥ 3 . In addition, the FNI was calculated in all patients with available data for descriptive purposes and to further characterize the study population⁵².

The study was conducted in accordance with the Declaration of Helsinki and the principles of Good Clinical Practice. All participants provided written informed consent. The study was approved by the Ethics Committee of Lazio Area 2 (Study name: NICHOLAS; Registry No. 33.23 CET 2 CBM).

Clinical and laboratory assessment

All patients were evaluated in the morning after an overnight fast of at least 8 hours. A comprehensive medical assessment was performed, including family and personal medical history, current and past comorbidities, medication use, and lifestyle habits, such as smoking status, alcohol consumption, and physical activity.

All participants underwent a standardized clinical evaluation, including the measurement of anthropometric parameters (body weight, height, waist and hip circumferences), with calculation of body mass index (BMI).

Biochemical data were also collected, including liver enzymes and markers of liver function (AST, ALT, GGT, ALP, total and direct bilirubin, albumin, INR), complete blood count, lipid profile (total cholesterol, HDL cholesterol, triglycerides), glucose metabolism parameters (fasting plasma glucose and glycated hemoglobin), and, when available, iron metabolism parameters (ferritin, transferrin, and serum iron).

Sample collection and electronic multi-sensing analysis

All recruited patients underwent blood, breath, urine, and saliva sampling. The e-nose and e-tongue used in this study are part of the BIONOTE system.

Breath samples were collected using the Pneumopipe® device (European Patent No. 12425057.2), developed by the Campus Bio-Medico University, and stored in absorbent cartridges (Tenax GR, Supelco) at $-20\text{ }^{\circ}\text{C}$ for at least two weeks before analysis with the BIONOTE electronic nose system. Breath analysis was performed through four consecutive measurements at increasing temperatures ($50\text{ }^{\circ}\text{C}$, $100\text{ }^{\circ}\text{C}$, $150\text{ }^{\circ}\text{C}$, and $200\text{ }^{\circ}\text{C}$), achieved by liquid nitrogen-based thermal desorption.

Urine samples were collected in cuvettes and subsequently analyzed using the BIONOTE electronic tongue system. Saliva samples were collected using cotton swabs, centrifuged at 1,000 rpm for 2 minutes, and, after dilution in distilled water at a 6.5:1 ratio, analyzed with the BIONOTE electronic tongue.

Blood samples were collected for serum separation, and serum aliquots were stored at $-80\text{ }^{\circ}\text{C}$ until analysis.

Statistical analysis

The main characteristics of the study sample were reported as mean \pm standard deviation or median and interquartile range for continuous variables, and as absolute number and percentage for categorical variables.

To assess the predictive value of e-nose and e-tongue analysis on urine (U*) or saliva (S*) for the different parameters of interest, we implemented a supervised classification approach based on elastic net–regularized logistic regression. Only observations with complete outcome data were included in the analysis. Sensor responses with zero variance were removed, and the remaining predictors were standardized (centered and scaled). No imputation of missing predictor values was performed; preprocessing steps were applied within each resampling iteration to prevent information leakage.

Elastic net regression was selected because of its ability to handle highly correlated sensor signals, reduce overfitting in high-dimensional datasets, and provide stable and interpretable models. These properties are particularly advantageous in e-sensing applications, characterized by a large number of interdependent features and relatively limited sample sizes.

Model performance was evaluated using 10-fold stratified cross-validation, preserving the outcome class distribution across folds. Hyperparameter tuning was conducted within the same cross-validation framework by jointly optimizing the elastic net mixing parameter (α), which controls the balance between ridge and lasso penalization, and the regularization parameter (λ). The optimal model configuration was selected by maximizing the mean cross-validated area under the receiver operating characteristic curve (AUC).

Classification performance was summarized by the cross-validated AUC. Additionally, out-of-fold class predictions were used to construct a confusion matrix and to derive standard classification metrics, including accuracy, sensitivity, specificity, positive predictive value (PPV), and negative predictive value (NPV), using an optimal threshold probability based on the maximization of the Youden Index.

Based on an estimated prevalence of fibrotic MASH of 15% and 35% in the non-invasive and histological cohorts, respectively, enrollment of at least 52 subjects in the non-invasive cohort and 19 subjects in the histological cohort was required to detect a minimum AUROC of 0.80, with a type I error (α) of 0.05 and 80% statistical power.

All the analyses were performed using R version 4.2.0 (R Foundation for Statistical Computing, Vienna, Austria).

Results

Characteristics of the study cohort

After the exclusion of two patients with coexisting liver disease, 215 patients were included in the study, of whom 158 belonged to the non-invasive cohort and 57 to the histological cohort. The main characteristics of the overall population and of each cohort separately are summarized in Table 2.

The study population was predominantly male (65%), with a mean age of 56.6 ± 13.9 years. The median body mass index was 31.1 kg/m^2 (interquartile range [IQR], 28.0–34.3), consistent with an obese phenotype. Despite comparable median BMI between the two cohorts (31.3 vs 30.8 kg/m^2), the prevalence of obesity ($\text{BMI} \geq 30$) was higher in the non-invasive cohort (57.6% vs 47.4%). Cardiometabolic comorbidities were highly prevalent. Arterial hypertension was present in 114 patients (54%), type 2 diabetes mellitus in 66 (31.4%), and dyslipidemia in 146 (69.5%), while cardiovascular disease was observed in 10 patients (5%). These conditions were more frequently observed in the histological cohort, particularly arterial hypertension (66.7% vs. 49.7%) and type 2 diabetes mellitus (38.6% vs. 29%). Overall, 111 of 210 patients (53%) had more than two metabolic risk factors, and 42 of 210 (20%) had more than three, with higher proportions in the histological cohort. A small proportion of patients (7, 3%) had chronic respiratory diseases (asthma or COPD), 4 in noninvasive cohort and 3 in histological cohort; given the low prevalence, they were not excluded from the analyses and no sensitivity analysis was performed.

Ultrasound assessment was available in 198 patients (92%). According to the Hamaguchi score, most individuals exhibited moderate (48%) or severe (43%) steatosis, with similar distributions across cohorts. Consistently, the median CAP was 302 dB/m (IQR 270–336), indicating a high burden of hepatic steatosis.

Biochemical data were available for most patients; missing values were present for some variables and were excluded from descriptive analyses. Serum liver enzymes were higher in the histological cohort, whereas metabolic parameters, including fasting glucose, HbA1c, lipid profile, and triglycerides, were broadly comparable between groups.

Characteristics	Overall	Noninvasive	Histological
	N=215	N=158	N=57
Sex, male	139 (65%)	105(66.5%)	34 (59.6%)
Age, years	56.6 (13.9)	55.5 (14.7)	59.7 (10.8)
Body Mass Index, kg/m ²	31.1 (28-34.3)	31.1 (28-34)	30.8 (27.9-34.7)
Cardiovascular disease, n (%)	10 (5%)	6 (3.9%)	4 (7%)
Arterial hypertension, n (%)	114 (54%)	76 (49.7%)	38 (66.7%)
Type 2 diabetes mellitus, n (%)	66 (31.4%)	44 (29%)	22 (38.6%)
Dyslipidemia, n (%)	146 (69.5%)	106 (69%)	40 (70.2%)
CAP, dB/m	302 (270-336)	300.5 (268-330)	308.5 (273-349)
US Hamaguchi score	198 (92%)	147(93%)	51 (89%)
Absent	2 (1%)	0 (0%)	2 (3.9%)
Mild	16 (8%)	10 (6.8%)	6 (11.8%)
Moderate	95 (48%)	72 (49%)	23 (45%)
Severe	85 (43%)	65 (44%)	20 (39%)
AST, U/L	32 (25-45)	29 (24-37.3)	43 (33-58)
ALT, U/L	43 (28-70)	37 (24-60.3)	64 (40.5-79)
GGT, U/L	40 (26-66)	36 (23-61)	53 (37-79.8)
ALP U/L	75 (62-93)	74 (64-91)	77.5 (58-96)
Glycemia, mg/dl	95 (88-106)	95 (88-105)	96 (87.5-113)
HbA1c, %	5.7 (5.3-6.1)	5.7 (5.3-6.1)	5.68 (5.3-6.3)
Cholesterol, mg/dl	169 (144-195)	176.5 (145-196)	156.5 (141-187)
HDL Chol, mg/dl	43.5 (38-52)	44 (38-53)	41.5 (37-49)
Tryglicerides	119 (86-156)	122.5 (92.7-159)	112 (82.5-146)

Table 2. Main characteristics of the study population.

Data reported as median (interquartile range) or mean (standard deviation) in case of continuous variables or as numbers with percentages in case of categorical variables. Kg= kilograms; m=metres; CAP= controlled attenuation parameter; dB= decibel; US=ultrasound; ALT= alanine transaminase; AST= aspartate aminotransferase; GGT= gamma-glutamyl transferase; ALP= alkaline phosphatase.

Disease severity assessment

In the non-invasive cohort, disease severity was assessed using non-invasive tools for fibrosis (LSM) and fibrotic MASH (FNI and FAST score) (table 3). In the histological cohort, disease severity was evaluated based on fibrosis stage and the NAFLD Activity Score (table 4).

Liver stiffness measurement was available for 210 patients and showed higher values in the histological cohort than in the non-invasive cohort (median 8.75 vs. 5.8 kPa). Overall, 51 patients (24.5%) had LSM values ≥ 8 kPa and 28 (13.4%) ≥ 10 kPa, with a markedly higher prevalence of subjects above both thresholds in the histological cohort. Specifically, 36 patients (64%) in the histological cohort had LSM values > 8 kPa, compared with 15 patients (9%) in the non-invasive cohort, while 23 patients (41%) had LSM values > 10 kPa, compared with 5 patients (3%).

The FNI score was available for 141 patients (88 in the non-invasive cohort and 53 in the histological cohort). Overall, 61 patients fulfilled the FNI criteria for fibrotic MASH, with a higher positivity rate in the histological cohort (34/53) than in the non-invasive cohort (27/88). At the rule-out cut-off, 21 patients, all from the non-invasive cohort, showed low-risk values, whereas all patients in the histological cohort had FNI values above the rule-out threshold.

The FAST score was available for 195 patients (139 in the non-invasive cohort and 56 in the histological cohort). Overall, 16 patients met the FAST criteria for fibrotic MASH, of whom 12 belonged to the histological cohort. At the rule-out cut-off, 114 patients showed low-risk values (100 in the non-invasive cohort and 14 in the histological cohort), whereas 81 patients had values above the rule-out threshold (39/139 and 42/56 in the non-invasive and histological cohorts, respectively).

In the histological cohort, fibrotic MASH was identified in 28 of 57 patients. Significant and advanced fibrosis, defined as fibrosis stages ≥ 2 and ≥ 3 , respectively, were observed in 38 and 17 patients.

NITs	Overall = 215	Noninvasive =158	Histological =57
LSM available	N=208	N=152	N=56
LSM, kPa	6.1 (4.98-7.9)	5.8 (4.8-6.8)	8.75 (6.9-12.5)
LSM>8, n (%)	51 (24.5%)	15 (9.9%)	36 (64%)
LSM>10, n (%)	28 (13.4%)	5 (3%)	23 (41%)
FAST score available	N=195	N=139	N=56
≥ 0.67 , n (%)	16 (8.2)	4 (2.9)	12 (21.4)
≥ 0.35 , n (%)	81 (41.5)	39 (28.1)	42 (75)
≥ 0.35 & < 0.67 , n (%)	65 (33)	35 (25.2)	30 (53.6)
< 0.35 , n(%)	114 (58.5)	100 (71.9)	14 (25)
NA, n (%)	20 (9.3)	19 (12)	1 (1.7)
FNI score available	N=141	N = 88	N=53
≥ 0.33 , n (%)	61 (43.3)	27 (30.7)	34 (64.1)
≥ 0.10 , n (%)	120 (85.1)	67 (76.1)	53 (100)
≥ 0.10 & < 0.33 , n (%)	59 (41.8)	40 (45.4)	19 (35)
< 0.10 , n (%)	21 (14.9)	21 (23.9)	0 (0)
NA, n (%)	17 (7.9)	70 (44)	4 (7)

Table 3. Non-invasive assessment of disease severity.

NITs=Non-Invasive Tools; N= number of patients; LSM = Liver Stiffness Measurement; NA=not available.

Histological Fibrotic MASH	N=57
NAS score ≥ 4 & F ≥ 2 , n (%)	28 (49.1)
NAS score < 4 and/or F < 2 , n(%)	29 (50.9)
NA	0

Table 4. Histological assessment of fibrosis stage and disease activity.

MASH = metabolic dysfunction- associated steatohepatitis; NAS = NAFLD activity score; F = fibrosis stage; N= number of patients; NA= not available.

Diagnostic performance of electronic multi-sensing technologies for fibrotic MASH and advanced fibrosis.

Exhaled breath, urine, and saliva samples were suitable for analysis in 195, 207, and 205 patients, respectively. Of these, breath samples were available for 155 patients in the non-invasive cohort and 40 in the histological cohort, urine samples for 153 and 54 patients, and saliva samples for 154 and 51 patients, respectively. The performance of the electronic nose (e-nose) and electronic tongue (e-tongue) was assessed for identifying fibrotic MASH, defined by the FAST score or histological criteria, and significant or advanced fibrosis, defined by LSM or histological stage. Complete performance metrics are presented in Tables 5 and 6 for the overall cohort (assessed by FAST score and LSM) and the biopsy-proven cohort (assessed by histological criteria), respectively.

Sample	Test	Accuracy	Sensitivity	Specificity	PPV	NPV	AUC
N	FAST	0,61	0,47	0,71	0,54	0,65	0,56
N	LSM \geq 8	0,52	0,71	0,47	0,28	0,85	0,56
N	LSM \geq 10	0,46	0,89	0,4	0,17	0,96	0,65
U	FAST	0,62	0,38	0,78	0,52	0,66	0,54
U	LSM \geq 8	0,75	0,44	0,84	0,47	0,83	0,63
U	LSM \geq 10	0,74	0,6	0,76	0,28	0,93	0,65
S	FAST	0,66	0,45	0,81	0,62	0,68	0,6
S	LSM \geq 8	0,69	0,62	0,71	0,39	0,86	0,6
S	LSM \geq 10	0,6	0,84	0,56	0,22	0,96	0,66

Table 5. Performance metrics of electronic multi-sensing technologies for fibrotic MASH and advanced fibrosis, as defined by FAST score and liver stiffness measurement, in the overall cohort.

Values are reported as absolute values. N= breath analysis by e-nose; U = urine analysis by e-tongue; S = saliva analysis by e-tongue; LSM = Liver Stiffness Measurement; PPV= positive predictive value; NPV = negative predictive value; AUC = area under the receiver operating characteristic curve.

Sample	Outcome	Accuracy	Sensitivity	Specificity	PPV	NPV	AUC
N	Fibrotic MASH	0,74	0,68	0,83	0,87	0,62	0,78
N	F \geq 2	0,74	0,74	0,75	0,89	0,5	0,7
N	F \geq 3	0,61	0,55	0,65	0,46	0,72	0,54
U	Fibrotic MASH	0,61	0,43	0,75	0,59	0,62	0,54
U	F \geq 2	0,65	0,66	0,63	0,75	0,52	0,57
U	F \geq 3	0,65	0,5	0,7	0,39	0,79	0,56
S	Fibrotic MASH	0,61	0,62	0,6	0,6	0,62	0,53
S	F \geq 2	0,53	0,53	0,53	0,68	0,38	0,43
S	F \geq 3	0,59	0,79	0,51	0,39	0,86	0,61

Table 5. Performance metrics of electronic multi-sensing technologies for fibrotic MASH and advanced fibrosis, as defined by histological criteria, in the biopsy-proven cohort.

Values are reported as absolute values. N= breath analysis by e-nose; U = urine analysis by e-tongue; S = saliva analysis by e-tongue; LSM = Liver Stiffness Measurement; PPV= positive predictive value; NPV = negative predictive value; AUC = area under the receiver operating characteristic curve.

Prediction of fibrotic MASH according to the FAST score

The diagnostic performance of the e-nose (breath analysis) and e-tongue (urine and saliva analysis) in predicting fibrotic MASH, as defined by the FAST score, was evaluated using a cut-off value of 0.35 ($\text{FAST} \geq 0.35$ Vs < 0.35). The e-nose achieved a moderate accuracy of 0.61, with low sensitivity and moderate specificity (AUC = 0.56). The urine-based e-tongue showed similar accuracy of 0.62 with limited sensitivity (AUC = 0.54), whereas the saliva-based e-tongue demonstrated slightly higher accuracy of 0.66 and specificity, although discrimination remained modest (AUC = 0.60). Overall, both technologies showed limited ability to predict fibrotic MASH as defined by the FAST score.

Prediction of significant fibrosis according to LSM

Using an LSM cut-off of 8 kPa, the e-nose showed low diagnostic accuracy (0.52) and limited discrimination (AUC = 0.56). The urine-based e-tongue achieved moderate accuracy (0.75) and modest discrimination (AUC = 0.63), while the saliva-based e-tongue showed intermediate performance (accuracy = 0.69; AUC = 0.60). The use of a higher cut-off (10 kPa) did not substantially improve overall diagnostic accuracy for any of the devices. Overall, these findings indicate modest performance in predicting fibrosis as defined by liver stiffness measurements.

Performance in the biopsy-proven cohort

In the histological cohort, the electronic nose showed moderate accuracy in identifying fibrotic MASH (0.74), correctly classifying 23 of 31 subjects, with high specificity

(0.83), a high positive predictive value (0.87), and good discrimination (AUC = 0.78). Similarly, significant fibrosis was identified with moderate accuracy and specificity (0.74 and 0.75, respectively), a high positive predictive value (0.89), and moderate discrimination (AUC = 0.70).

In contrast, urine- and saliva-based electronic tongue analyses showed lower and more variable performance, with modest accuracy for fibrotic MASH (0.61 for both matrices) and modest to low accuracy for significant fibrosis (0.65 and 0.53, respectively), showing limited discriminatory ability for both outcomes. Overall, diagnostic performance in the biopsy-proven cohort, although modest, was higher than that observed in the non-invasive assessment.

Comparative performance of FAST and LSM in biopsy-proven disease

Given the better performance of electronic technologies in the biopsy-proven cohort compared with analyses based on indirect non-invasive markers (FAST score and LSM), we further evaluated the accuracy of these markers within the biopsy-proven cohort. Complete performance metrics are reported in Table 7. Accuracy and ROC curves are reported in Figure 7 and 8, respectively.

In predicting fibrotic MASH, the FAST score at a threshold of 0.35 showed modest diagnostic accuracy (0.71), with high sensitivity (0.96), high NPV (0.93), and good discrimination (AUC = 0.81). Conversely, when using a higher threshold of 0.67 (FAST-in), it was characterized by moderate accuracy (0.64) and discrimination (AUC = 0.64).

With respect to histological fibrosis, LSM with a cut-off of ≥ 8 kPa showed modest accuracy (0.61) and limited discrimination (AUC = 0.64). Increasing the threshold to ≥ 10 kPa resulted in moderate accuracy (0.68) and discrimination (AUC = 0.77).

Overall, in the biopsy-proven cohort, FAST score and LSM demonstrated moderate accuracy, with FAST showing slightly better diagnostic performance and discriminatory ability.

Test	Outcome	Sensitivity	Specificity	PPV	NPV	Accuracy
LSM ≥ 8	F ≥ 2	0.684	0.444	0.722	0.4	0.607
LSM ≥ 10	F ≥ 3	0.647	0.692	0.478	0.818	0.679
FAST	fibrotic MASH	0.964	0.464	0.643	0.929	0.714
FASTin	fibrotic MASH	0.357	0.929	0.833	0.591	0.643

Table 7. Performance metrics of FAST and liver stiffness measurement for fibrotic MASH and advanced fibrosis in the histological cohort.

LSM = Liver Stiffness Measurement; PPV= positive predictive value; NPV = negative predictive value.

Diagnostic Accuracy of Non-Invasive Tests

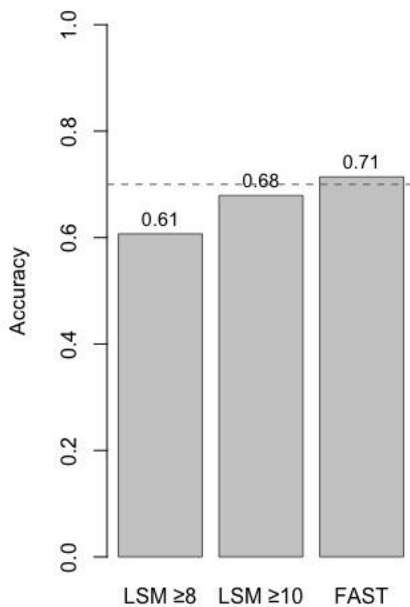


Figure 7. Comparison of diagnostic accuracy of FAST and liver stiffness measurement for fibrotic MASH and significant or advanced fibrosis in the biopsy-proven cohort. LSM = Liver Stiffness Measurement.

ROC curves (histological cohort)

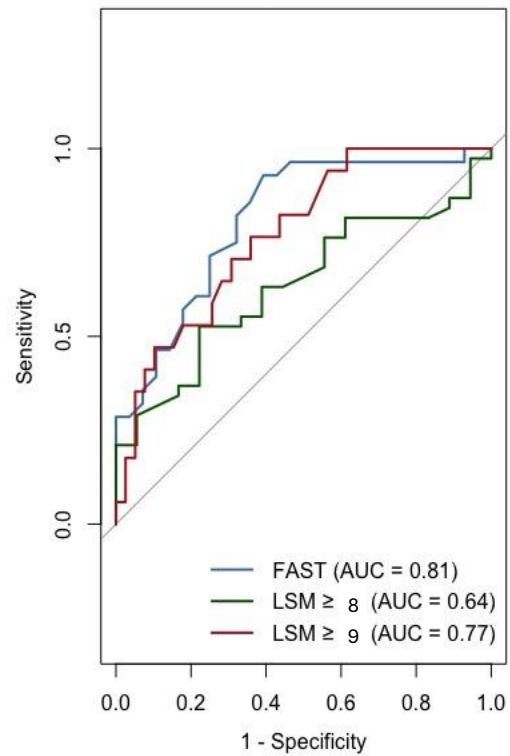


Figure 8. Comparative area under the receiver operating characteristic (AUC) curve of FAST and liver stiffness measurement for fibrotic MASH and significant or advanced fibrosis in the biopsy-proven cohort. LSM = Liver Stiffness Measurement.

Discussion

In the present substudy, multisensory electronic technologies demonstrated overall modest or, at the best, moderate diagnostic performance in identifying patients with fibrotic MASH and significant fibrosis across different analytical settings. However, in the histological cohort, encouraging results were observed for the electronic nose, which appeared to perform better than FAST, with higher accuracy in identifying fibrotic MASH and significant fibrosis. Moreover, whereas FAST was characterized by high sensitivity and negative predictive value, supporting its potential role as a screening tool, the electronic nose showed high specificity and positive predictive value, suggesting a possible role in confirming disease.

While histological assessment remains the gold standard for the diagnosis of steatosis, fibrosis, and MASH, its routine use in clinical practice has progressively declined^{3,4,34}. As a result, substantial efforts have been devoted to the development of non-invasive tools for the identification of significant fibrosis and fibrotic MASH³⁴. However, currently available composite scores and imaging-based approaches show variable performance and are frequently limited by cost, complexity, and restricted availability in specialized centers^{2,29,38}.

In recent years, multisensory analysis techniques have emerged as promising non-invasive tools applicable to a wide range of pathological conditions, including chronic liver diseases^{63–65,70}. This approach is grounded in the concept that pathological processes are associated with the production and release of abnormal metabolites, which may serve as disease biomarkers and can be detected in blood, biological fluids, tissues, or exhaled breath^{64,71}. Given the central role of the liver in systemic metabolic regulation, chronic liver disease is likely to induce qualitative and quantitative alterations in metabolic profiles, leading to modified patterns of metabolites excreted through gases and body fluids.

To our knowledge, this is the first large-scale study in a MASLD population to evaluate multisensory electronic devices, including electronic nose and electronic tongue, for the identification of fibrotic MASH or significant fibrosis, which represent the most clinically relevant and treatment-eligible forms of the disease.

In the context of MASLD, available evidence on the use of electronic sensory technologies remains limited. Previous studies have mainly relied on conventional analytical approaches for breath analysis, while only preliminary data from proof-of-concept investigations have explored the potential of electronic nose systems for disease discrimination and risk stratification^{71–73}.

A previous study based on breath analysis using gas chromatography–mass spectrometry (GC-MS) in a histologically characterized cohort demonstrated that the analysis of volatile organic compounds (VOCs) in exhaled breath allowed the identification of specific compounds capable of discriminating patients with and without NASH, with an AUC of 0.77 ± 0.07 . This approach showed higher accuracy than conventional biomarkers, such as transaminases and the AST/ALT ratio, and substantially lower misdiagnosis rates⁷². Similarly, Sinha et al. identified specific VOC profiles able to discriminate healthy subjects, non-cirrhotic NAFLD, and NAFLD cirrhosis, with excellent diagnostic performance, particularly for cirrhosis (AUROC up to 0.94–0.98)⁷¹. More recently, the same group applied electronic nose technology to breath VOC profiling in MASLD patients, demonstrating clear separation between disease stages and identifying distinct patient clusters with different risks of progression, with moderate-good prognostic accuracy (AUC = 0.78)⁷³. However, these findings should be interpreted with caution, as they were derived from an exploratory study with relatively small sample sizes.

Our results, obtained from a cohort of 215 patients with MASLD, further support the potential role of electronic sensing technologies in risk stratification in chronic liver disease. Unlike previous investigations, which mainly focused on breath VOC

analysis⁷⁴⁻⁷⁷, our study extended this approach to electronic tongue devices using urine and saliva samples.

Overall, among the two systems (e-nose and e-tongue) and the three biological matrices analyzed (breath and urine and saliva), the electronic nose showed the highest diagnostic accuracy, particularly in identifying patients with histologically defined fibrotic MASH and significant fibrosis. The electronic nose achieved an accuracy of 0.74 for both outcomes, with moderate-to-good discrimination. In contrast, urine- and saliva-based electronic tongue analyses showed lower and more variable performance, with the exception of urine-based analysis, which achieved moderate accuracy in identifying significant fibrosis despite limited discrimination.

Although overall diagnostic performance was moderate, a better performance of electronic technologies was observed in the biopsy-proven cohort compared with analyses based on indirect non-invasive markers. While median BMI was comparable between groups, patients assessed using non-invasive methods showed a higher prevalence of obesity than those assessed histologically, a difference that should be considered when interpreting these between-group findings. Overall, these observations suggest that the assessment of diagnostic accuracy may be influenced, at least in part, by the reference standard used. Accordingly, we further evaluated the performance of FAST and liver stiffness measurement within the histological cohort. In this subgroup, liver stiffness thresholds of ≥ 8 and ≥ 10 kPa showed modest accuracy and limited discrimination for the identification of significant and advanced fibrosis, respectively, whereas the FAST score demonstrated better, although still moderate-to-good, diagnostic performance (AUC of 0.81). While FAST performance was consistent with previous reports⁵⁸⁻⁶⁰, liver stiffness measurement showed lower discrimination, particularly for significant fibrosis, possibly reflecting the influence of patient-related and technical factors as well as the stringent histological reference standard.

Notably, in the histological cohort, FAST at the rule-out threshold of 0.35 confirmed high sensitivity and negative predictive value, supporting its role as a screening tool⁵⁸⁻

⁶⁰. Conversely, our results for the electronic nose showed high specificity and positive predictive value, suggesting potential utility in identifying patients at high risk.

This study has several limitations. Its current single-center setting may limit the generalizability of the findings, although recruitment is ongoing at an additional center. In addition, despite the prospective design, the incomplete availability of laboratory data and the technical infeasibility of collecting some biological samples or performing some non-invasive assessments represent a limitation that reflects real-world clinical practice. Moreover, the applied multisensory technologies detect metabolic patterns without identifying individual metabolites. Integration with metabolomic analyses may improve biological interpretability and clinical applicability. Therefore, future evaluation in independent cohorts and complementary metabolomic analyses would be valuable.

Notably, in our study, analyses performed in the histological cohort demonstrated diagnostic performance comparable to FAST in identifying patients with fibrotic MASH and superior to liver stiffness measurement in detecting significant fibrosis.

Importantly, the performance of e-sensing systems was obtained using a standalone approach, without integration of clinical, biochemical, or imaging variables. The information captured by multisensory technologies may provide additional value when incorporated into multivariable predictive models. Indeed, most validated non-invasive algorithms for MASLD rely on the integration of heterogeneous biological signals.

Moreover, the rapidity, scalability, and low operational cost of e-sensing technologies represent major advantages for targeted and confirmatory strategies and longitudinal monitoring, where moderate diagnostic accuracy may be offset by high feasibility and repeated measurements over time.

In this context, the results of the present study support the potential role of e-sensing-derived features as novel components of integrated risk stratification strategies rather than as isolated diagnostic tools. Building on these findings, future studies will focus

on the development and validation of integrated predictive models combining e-sensing data with established clinical and biochemical parameters, with the aim of improving individualized risk assessment and identifying patients most likely to benefit from targeted interventions.

In parallel, complementary metabolomic analyses will be pursued to characterize the molecular signatures underlying sensor-derived patterns, enhance their biological interpretability, and evaluate their association with severe liver disease and hepatic outcomes.

Furthermore, future studies may evaluate longitudinal assessments to estimate the impact of lifestyle and therapeutic interventions on sensor-derived metabolic patterns.

In conclusion, while this thesis primarily reports the results of the first substudy, it also lays the foundation for the development of predictive models and metabolomic analyses aimed at exploring the biological and potential prognostic relevance of e-sensing-derived signatures, which are currently under investigation.

2.2

Development of a multisensory electronic technology-based predictive model for risk stratification and identification of fibrotic MASH and significant or advanced fibrosis

In the first substudy, electronic multisensory technologies, particularly the e-nose, showed a moderate predictive performance in the histological cohort (accuracy 0.74; AUC 0.78). Building on these findings, this substudy is grounded in the hypothesis that integrating a limited set of robust e-sensory patterns with routinely available clinical and biochemical variables into a composite predictive model may improve diagnostic performance. Accordingly, the present study aims to develop a predictive model combining one or more e-sensing–derived features with clinical and biochemical variables to improve risk stratification, particularly for the identification of patients with fibrotic MASH and significant fibrosis.

The histological cohort will represent the primary derivation cohort, as this setting showed the best performance of e-sensory technologies. Inclusion and exclusion criteria, as well as the definitions of fibrotic MASH and significant fibrosis, were consistent with those described in the first substudy. This substudy focuses on the subgroup of patients undergoing liver biopsy, resulting in a more selected population.

First, we will identify the most informative olfactory and taste-related patterns associated with fibrotic MASH and significant fibrosis using supervised statistical learning approaches. These features will represent the innovative e-sensory predictors included in the model. In parallel, a set of 14 routinely available clinical and laboratory variables, selected based on previous literature, will be included as traditional predictors: age, sex, BMI, waist circumference, glucose, hemoglobin A1c (HbA1c), total cholesterol, HDL cholesterol, triglycerides, aspartate aminotransferase (AST), alanine aminotransferase, gamma-glutamyltransferase, platelet count, albumin, and total bilirubin. Candidate e-sensory and clinical predictors will be entered into a bootstrapped stepwise logistic regression model, in which model development and

feature selection will be performed within the resampling framework, to derive an interpretable predictive score. The final model will be subsequently tested and externally validated in independent cohorts to assess its generalizability.

Model performance will be initially assessed in the derivation cohort using the area under the receiver operating characteristic curve (AUROC). Rule-out and rule-in cutoffs will be derived in the derivation cohort based on sensitivity and specificity, with the aim of optimizing clinical rule-in and rule-out performance. At each cutoff, sensitivity, specificity, positive predictive value (PPV), and negative predictive value (NPV) will be calculated, together with their 95% confidence intervals (CIs). External validation will be used to confirm model performance and robustness in independent cohorts.

To date, 57 patients were enrolled in the histological cohort, with breath samples available for 40 patients, urine samples for 54 patients, and saliva samples for 51 patients, respectively. Complete laboratory tests were available for 56 of 57 patients.

At this stage, this substudy is conceived as an exploratory investigation in a relatively limited cohort. On the basis of these preliminary findings, the cohort will be expanded by enrolling additional participants to improve model robustness and enable subsequent validation in independent external cohorts.

2.3

Identification of metabolomic signatures associated with multisensory electronic technology-based assessment of fibrotic MASH and severe liver disease

Multisensory electronic techniques are based on the premise that pathological processes induce alterations in metabolic activity, resulting in modified metabolite profiles detectable in biological matrices^{64,71}. Given the central role of the liver in metabolic processes, MASLD is expected to generate disease-specific metabolic signatures reflected in characteristic patterns of volatile and soluble compounds.

As described in the Methods of the first substudy, electronic multisensory systems rely on arrays of non-selective gas or liquid sensors that mimic human sensory perception⁶⁶. Although these systems are able to recognize distinct patterns, or “fingerprints,” associated with specific pathological conditions, they do not permit the identification of individual metabolites⁶³.

Based on this background, this substudy is grounded in the hypothesis that sensor-derived patterns may correspond to specific metabolomic signatures.

Specifically, the present study aims to evaluate the association between e-sensing–derived fingerprints and serum metabolomic profiles in patients with and without fibrotic MASH or significant fibrosis. Furthermore, the study aims to assess whether e-sensing–based metabolomic profiling is associated with an increased risk of incident severe liver disease, thereby evaluating their potential prognostic value.

To achieve these objectives, fasting serum samples were collected from subgroups of individuals enrolled in both the non-invasive and histological cohorts. Inclusion and exclusion criteria, as well as the definitions of fibrotic MASH and significant fibrosis, were consistent with those described in the first substudy.

Serum metabolomics has been quantified using the nuclear magnetic resonance (NMR)-based Nightingale assay platform (Nightingale Health Plc, Helsinki, Finland).

Based on our cohort, we will derive metabolomic signatures for fibrotic MASH and significant fibrosis associated with the e-sensing–derived fingerprints.

The metabolomic signatures, identified in our cohort, will subsequently be evaluated in 120,000 individuals from the UK Biobank study with metabolomics data available and quantified using the same platform, as an external validation step.

The UK Biobank is a large population-based study including more than 500,000 participants with standardized clinical, anthropometric, and laboratory data. In a subset of approximately 120,000 participants, metabolomics data are available. Medical diagnoses have been obtained through linkage with hospital admissions, death registers, and cancer registries⁷⁸.

In the UK Biobank, we will assess whether metabolomic signatures associated with e-sensing fingerprints are associated with fibrotic MASH assessed by liver magnetic resonance imaging (MRI). Consistent with previously reported MRI-based phenotyping approaches^{52,79}, fibrotic MASH will be defined as proton density fat fraction >5.5%, iron-corrected T1 >800 ms, and Fibrosis-4 Index ≥ 1.3 . In addition, we will evaluate whether these metabolomic patterns are associated with the risk of incident severe liver disease. Severe liver disease is defined as a composite outcome including cirrhosis, decompensated liver disease, hepatocellular carcinoma, and liver transplantation.

Comparisons of metabolomic species between individuals with and without fibrotic MASH will be performed using linear regression models adjusted for age, sex, and BMI. Associations with fibrotic MASH in the UK Biobank will be evaluated using similar models. Associations with incident severe liver disease will be estimated using Cox proportional hazards models. All statistical analyses will be conducted using R version 4.2.0 (R Foundation for Statistical Computing, Vienna, Austria).

To date, serum samples from 152 patients were collected, including 124 from the non-invasive cohort and 28 from the histological cohort. Serum samples were subjected to

comprehensive metabolomic profiling using the Nightingale NMR platform, providing quantitative data on approximately 250 biomarkers involved in multiple metabolic pathways, including insulin resistance, immune regulation, inflammation, and oxidative stress. The panel includes detailed measures of lipoprotein subclasses, circulating fatty acids (saturated and unsaturated), amino acids (branched-chain and aromatic), and glycolysis-related metabolites.

In conclusion, by integrating e-sensing–derived fingerprints with serum metabolomic profiles, this is expected to identify reproducible metabolic signatures associated with fibrotic MASH and significant fibrosis. These findings may support the biological interpretation of e-sensing–based models and contribute to the identification of novel biomarkers for disease risk stratification.

3. Conclusion and future perspective

While this thesis primarily reports the results of the first substudy, it also establishes the conceptual and methodological framework for the second and third substudies, which are currently ongoing and will be addressed in future work.

The increasing prevalence of MASLD represents a growing global health burden. MASLD is characterized by marked clinical heterogeneity, with only a subset of patients developing progressive disease and adverse liver-related outcomes. In particular, individuals with fibrotic MASH and significant or advanced fibrosis are at substantially increased risk of disease progression and represent priority candidates for referral to specialized liver clinics and for enrollment in clinical trials or treatment with recently approved therapies.

The timely identification of these high-risk patients is therefore crucial for targeting care and healthcare resources. Currently, available diagnostic strategies remain limited by invasiveness, cost, restricted availability, and variable performance across populations.

Multisensory electronic technologies have recently emerged as a promising non-invasive tool, offering rapid, low-cost assessment across a wide range of pathological condition, including chronic liver disease, by capturing disease-specific “fingerprints” in biological matrices.

This thesis provides evidence that multisensory electronic technologies exhibit moderate but clinically meaningful performance in the non-invasive identification of patients with fibrotic MASH and significant fibrosis. In particular, the first substudy showed that e-nose–based assessment may complement existing diagnostic tools. In the biopsy-proven cohort, e-nose breath analysis appeared to perform better than widely used non-invasive tools, including FAST and liver stiffness measurement, in identifying patients with fibrotic MASH and significant fibrosis. Notably, the e-nose showed high specificity and positive predictive value, whereas FAST was

characterized by high sensitivity and negative predictive value. In this context, e-nose-based assessment may represent a valuable confirmatory approach for identifying patients at increased risk.

Building on these findings, the second and third substudies aim to further refine risk stratification strategies through predictive modeling, integrating data from different multisensory e-technologies and clinical-biochemical variables, as well as through metabolomic integration. Although these projects are still ongoing, they represent important steps toward improving individualized assessment and prognostic evaluation in MASLD. Together, these studies represent the planned continuation of this research project and aim to further advance the development of e-sensing-based tools for precision risk stratification in MASLD.

Overall, this work supports the potential role of multisensory electronic technologies as scalable and complementary tools within integrated diagnostic and prognostic frameworks.

Finally, recent evidence recognizes the utility of non-invasive tests for monitoring disease progression and response to therapy. A major advantage of these methods, compared with liver biopsy, is their ability to be easily and repeatedly applied over time to monitor patients. Moreover, in the context of emerging pharmacological therapies, non-invasive tools are increasingly required to track treatment response and disease evolution.

As a future perspective, we plan to develop a study to assess the potential of e-sensing technologies for longitudinal monitoring of patients, with particular emphasis on evaluating the impact of interventional strategies on sensor-derived patterns associated with fibrotic MASH and significant or advanced fibrosis. Specifically, a cohort of MASLD patients with fibrotic MASH or significant fibrosis will be re-evaluated one year after baseline assessment, following a lifestyle modification program or any treatment. Participants will undergo repeated clinical, biochemical, Fibroscan® and electronic nose and tongue assessment to determine the impact of these interventions

on e-sensing–derived biomarkers and metabolic clusters related to disease activity and fibrosis stage.

References

1. Younossi ZM, Golabi P, Paik JM, et al. The global epidemiology of nonalcoholic fatty liver disease (NAFLD) and nonalcoholic steatohepatitis (NASH): a systematic review. *Hepatology* 2023;77:1335-1347.
2. Tantu MT, Farhana FZ, Haque F, et al. Pathophysiology, noninvasive diagnostics and emerging personalized treatments for metabolic associated liver diseases. *npj Gut Liver* 2025;2:18.
3. Tacke F, Horn P, Wai-Sun Wong V, et al. EASL–EASD–EASO Clinical Practice Guidelines on the management of metabolic dysfunction-associated steatotic liver disease (MASLD). *Journal of Hepatology* 2024;81:492-542.
4. Huang DQ, Wong VWS, Rinella ME, et al. Metabolic dysfunction-associated steatotic liver disease in adults. *Nat Rev Dis Primers* 2025;11:14.
5. Rinella ME, Lazarus JV, Ratziu V, et al. A multisociety Delphi consensus statement on new fatty liver disease nomenclature. *Hepatology* 2023;78:1966-1986.
6. Kleiner DE, Brunt EM, Van Natta M, et al. Design and validation of a histological scoring system for nonalcoholic fatty liver disease†. *Hepatology* 2005;41:1313-1321.
7. Younossi ZM, Zelber-Sagi S, Lazarus JV, et al. Global Consensus Recommendations for Metabolic Dysfunction-Associated Steatotic Liver Disease and Steatohepatitis. *Gastroenterology* 2025;169:1017-1032.e2.
8. Younossi ZM. Non-alcoholic fatty liver disease – A global public health perspective. *Journal of Hepatology* 2019;70:531-544.
9. Quek J, Chan KE, Wong ZY, et al. Global prevalence of non-alcoholic fatty liver disease and non-alcoholic steatohepatitis in the overweight and obese population: a systematic review and meta-analysis. *The Lancet Gastroenterology & Hepatology* 2023;8:20-30.
10. Younossi ZM, Golabi P, Price JK, et al. The Global Epidemiology of Nonalcoholic Fatty Liver Disease and Nonalcoholic Steatohepatitis Among Patients With Type 2 Diabetes. *Clinical Gastroenterology and Hepatology* 2024;22:1999-2010.e8.
11. Lee EJ, Choi M, Ahn SB, et al. Prevalence of nonalcoholic fatty liver disease in pediatrics and adolescents: a systematic review and meta-analysis. *World J Pediatr* 2024;20:569-580.

12. Young S, Tariq R, Provenza J, et al. Prevalence and Profile of Nonalcoholic Fatty Liver Disease in Lean Adults: Systematic Review and Meta-Analysis. *Hepatol Commun* 2020;4:953-972.
13. Loomba R, Friedman SL, Shulman GI. Mechanisms and disease consequences of nonalcoholic fatty liver disease. *Cell* 2021;184:2537-2564.
14. Byrne CD, Armandi A, Pellegrinelli V, et al. Metabolic dysfunction-associated steatotic liver disease: a condition of heterogeneous metabolic risk factors, mechanisms and comorbidities requiring holistic treatment. *Nat Rev Gastroenterol Hepatol* 2025;22:314-328.
15. Singh S, Allen AM, Wang Z, et al. Fibrosis Progression in Nonalcoholic Fatty Liver vs Nonalcoholic Steatohepatitis: A Systematic Review and Meta-analysis of Paired-Biopsy Studies. *Clinical Gastroenterology and Hepatology* 2015;13:643-654.e9.
16. Younossi ZM, Stepanova M, Rafiq N, et al. Pathologic criteria for nonalcoholic steatohepatitis: Interprotocol agreement and ability to predict liver-related mortality. *Hepatology* 2011;53:1874-1882.
17. Angulo P, Kleiner DE, Dam-Larsen S, et al. Liver Fibrosis, but No Other Histologic Features, Is Associated With Long-term Outcomes of Patients With Nonalcoholic Fatty Liver Disease. *Gastroenterology* 2015;149:389-397.e10.
18. Ekstedt M, Hagström H, Nasr P, et al. Fibrosis stage is the strongest predictor for disease-specific mortality in NAFLD after up to 33 years of follow-up. *Hepatology* 2015;61:1547-1554.
19. Hagström H, Nasr P, Ekstedt M, et al. Fibrosis stage but not NASH predicts mortality and time to development of severe liver disease in biopsy-proven NAFLD. *Journal of Hepatology* 2017;67:1265-1273.
20. Taylor RS, Taylor RJ, Bayliss S, et al. Association Between Fibrosis Stage and Outcomes of Patients With Nonalcoholic Fatty Liver Disease: A Systematic Review and Meta-Analysis. *Gastroenterology* 2020;158:1611-1625.e12.
21. Terracciani F, Falcomatà A, Gallo P, et al. Prognostication in NAFLD: physiological bases, clinical indicators, and newer biomarkers. *J Physiol Biochem* 2023;79:851-868.
22. Calzadilla Bertot L, Adams L. The Natural Course of Non-Alcoholic Fatty Liver Disease. *IJMS* 2016;17:774.
23. Schuppan D, Surabattula R, Wang XY. Determinants of fibrosis progression and regression in NASH. *Journal of Hepatology* 2018;68:238-250.

24. Eslam M, George J. Genetic contributions to NAFLD: leveraging shared genetics to uncover systems biology. *Nat Rev Gastroenterol Hepatol* 2020;17:40-52.
25. Trépo E, Valenti L. Update on NAFLD genetics: From new variants to the clinic. *Journal of Hepatology* 2020;72:1196-1209.
26. Eslam M, Valenti L, Romeo S. Genetics and epigenetics of NAFLD and NASH: Clinical impact. *Journal of Hepatology* 2018;68:268-279.
27. Kleiner DE, Brunt EM, Wilson LA, et al. Association of Histologic Disease Activity With Progression of Nonalcoholic Fatty Liver Disease. *JAMA Netw Open* 2019;2:e1912565.
28. Sanyal AJ, Castera L, Wong VW-S. Noninvasive Assessment of Liver Fibrosis in NAFLD. *Clinical Gastroenterology and Hepatology* 2023;21:2026-2039.
29. Stern C, Castera L. Identification of high-risk subjects in nonalcoholic fatty liver disease. *Clin Mol Hepatol* 2023;29:S196-S206.
30. Boursier J, Tsochatzis EA. Case-finding strategies in non-alcoholic fatty liver disease. *JHEP Reports* 2021;3:100219.
31. Sanyal AJ, Brunt EM, Kleiner DE, et al. Endpoints and clinical trial design for nonalcoholic steatohepatitis. *Hepatology* 2011;54:344-353.
32. Chen VL, Morgan TR, Rotman Y, et al. Resmetirom therapy for metabolic dysfunction-associated steatotic liver disease: October 2024 updates to AASLD Practice Guidance. *Hepatology* 2025;81:312-320.
33. Bansal MB, Patton H, Morgan TR, et al. Semaglutide therapy for metabolic dysfunction-associated steatohepatitis: November 2025 updates to AASLD Practice Guidance. *Hepatology* November 2025.
34. Rinella ME, Neuschwander-Tetri BA, Siddiqui MS, et al. AASLD Practice Guidance on the clinical assessment and management of nonalcoholic fatty liver disease. *Hepatology* 2023;77:1797-1835.
35. Mózes FE, Lee JA, Selvaraj EA, et al. Diagnostic accuracy of non-invasive tests for advanced fibrosis in patients with NAFLD: an individual patient data meta-analysis. *Gut* 2022;71:1006-1019.
36. Vilar-Gomez E, Chalasani N. Non-invasive assessment of non-alcoholic fatty liver disease: Clinical prediction rules and blood-based biomarkers. *Journal of Hepatology* 2018;68:305-315.

37. Heyens LJM, Busschots D, Koek GH, et al. Liver Fibrosis in Non-alcoholic Fatty Liver Disease: From Liver Biopsy to Non-invasive Biomarkers in Diagnosis and Treatment. *Front Med* 2021;8:615978.
38. Anstee QM, Castera L, Loomba R. Impact of non-invasive biomarkers on hepatology practice: Past, present and future. *Journal of Hepatology* 2022;76:1362-1378.
39. McPherson S, Stewart SF, Henderson E, et al. Simple non-invasive fibrosis scoring systems can reliably exclude advanced fibrosis in patients with non-alcoholic fatty liver disease. *Gut* 2010;59:1265-1269.
40. Angulo P, Hui JM, Marchesini G, et al. The NAFLD fibrosis score: A noninvasive system that identifies liver fibrosis in patients with NAFLD†. *Hepatology* 2007;45:846-854.
41. Guha IN, Parkes J, Roderick P, et al. Noninvasive markers of fibrosis in nonalcoholic fatty liver disease: Validating the European Liver Fibrosis Panel and exploring simple markers. *Hepatology* 2008;47:455-460.
42. Vali Y, Lee J, Boursier J, et al. Enhanced liver fibrosis test for the non-invasive diagnosis of fibrosis in patients with NAFLD: A systematic review and meta-analysis. *Journal of Hepatology* 2020;73:252-262.
43. Eddowes PJ, Sasso M, Allison M, et al. Accuracy of FibroScan Controlled Attenuation Parameter and Liver Stiffness Measurement in Assessing Steatosis and Fibrosis in Patients With Nonalcoholic Fatty Liver Disease. *Gastroenterology* 2019;156:1717-1730.
44. Siddiqui MS, Vuppalanchi R, Van Natta ML, et al. Vibration-Controlled Transient Elastography to Assess Fibrosis and Steatosis in Patients With Nonalcoholic Fatty Liver Disease. *Clinical Gastroenterology and Hepatology* 2019;17:156-163.e2.
45. Berzigotti A, Tsochatzis E, Boursier J, et al. EASL Clinical Practice Guidelines on non-invasive tests for evaluation of liver disease severity and prognosis – 2021 update. *Journal of Hepatology* 2021;75:659-689.
46. Imajo K, Kessoku T, Honda Y, et al. Magnetic Resonance Imaging More Accurately Classifies Steatosis and Fibrosis in Patients With Nonalcoholic Fatty Liver Disease Than Transient Elastography. *Gastroenterology* 2016;150:626-637.e7.
47. Hsu C, Caussy C, Imajo K, et al. Magnetic Resonance vs Transient Elastography Analysis of Patients With Nonalcoholic Fatty Liver Disease: A Systematic

Review and Pooled Analysis of Individual Participants. *Clinical Gastroenterology and Hepatology* 2019;17:630-637.e8.

48. Selvaraj EA, Mózes FE, Jayaswal ANA, et al. Diagnostic accuracy of elastography and magnetic resonance imaging in patients with NAFLD: A systematic review and meta-analysis. *Journal of Hepatology* 2021;75:770-785.
49. Sanyal AJ, Foucquier J, Younossi ZM, et al. Enhanced diagnosis of advanced fibrosis and cirrhosis in individuals with NAFLD using FibroScan-based Agile scores. *Journal of Hepatology* 2023;78:247-259.
50. Boursier J, Anty R, Vonghia L, et al. Screening for therapeutic trials and treatment indication in clinical practice: MACK -3, a new blood test for the diagnosis of fibrotic NASH. *Aliment Pharmacol Ther* 2018;47:1387-1396.
51. Canivet CM, Zheng M-H, Qadri S, et al. Validation of the Blood Test MACK-3 for the Noninvasive Diagnosis of Fibrotic Nonalcoholic Steatohepatitis: An International Study With 1924 Patients. *Clinical Gastroenterology and Hepatology* 2023;21:3097-3106.e10.
52. Tavaglione F, Jamialahmadi O, De Vincentis A, et al. Development and Validation of a Score for Fibrotic Nonalcoholic Steatohepatitis. *Clinical Gastroenterology and Hepatology* 2023;21:1523-1532.e1.
53. Harrison SA, Ratziu V, Boursier J, et al. A blood-based biomarker panel (NIS4) for non-invasive diagnosis of non-alcoholic steatohepatitis and liver fibrosis: a prospective derivation and global validation study. *The Lancet Gastroenterology & Hepatology* 2020;5:970-985.
54. Harrison SA, Ratziu V, Magnanensi J, et al. NIS2+™, an optimisation of the blood-based biomarker NIS4® technology for the detection of at-risk NASH: A prospective derivation and validation study. *Journal of Hepatology* 2023;79:758-767.
55. Zhou Y, Orešič M, Leivonen M, et al. Noninvasive Detection of Nonalcoholic Steatohepatitis Using Clinical Markers and Circulating Levels of Lipids and Metabolites. *Clinical Gastroenterology and Hepatology* 2016;14:1463-1472.e6.
56. Nouredin M, Truong E, Mayo R, et al. Serum identification of at-risk MASH: The metabolomics-advanced steatohepatitis fibrosis score (MASEF). *Hepatology* 2024;79:135-148.
57. Andersson A, Kelly M, Imajo K, et al. Clinical Utility of Magnetic Resonance Imaging Biomarkers for Identifying Nonalcoholic Steatohepatitis Patients at High Risk of Progression: A Multicenter Pooled Data and Meta-Analysis. *Clinical Gastroenterology and Hepatology* 2022;20:2451-2461.e3.

58. Newsome PN, Sasso M, Deeks JJ, et al. FibroScan-AST (FAST) score for the non-invasive identification of patients with non-alcoholic steatohepatitis with significant activity and fibrosis: a prospective derivation and global validation study. *The Lancet Gastroenterology & Hepatology* 2020;5:362-373.
59. Ravaioli F, Dajti E, Mantovani A, et al. Diagnostic accuracy of FibroScan-AST (FAST) score for the non-invasive identification of patients with fibrotic non-alcoholic steatohepatitis: a systematic review and meta-analysis. *Gut* 2023;72:1399-1409.
60. Malandris K, Arampidis D, Mainou M, et al. FibroScan-AST score for diagnosing fibrotic MASH: A systematic review and meta-analysis of diagnostic test accuracy studies. *J of Gastro and Hepatol* 2024;39:2582-2591.
61. Nouredin M, Truong E, Gornbein JA, et al. MRI-based (MAST) score accurately identifies patients with NASH and significant fibrosis. *Journal of Hepatology* 2022;76:781-787.
62. Jung J, Loomba RR, Imajo K, et al. MRE combined with FIB-4 (MEFIB) index in detection of candidates for pharmacological treatment of NASH-related fibrosis. *Gut* 2021;70:1946-1953.
63. Fitzgerald J, Fenniri H. Cutting Edge Methods for Non-Invasive Disease Diagnosis Using E-Tongue and E-Nose Devices. *Biosensors* 2017;7:59.
64. Wilson A. Advances in Electronic-Nose Technologies for the Detection of Volatile Biomarker Metabolites in the Human Breath. *Metabolites* 2015;5:140-163.
65. Tibaduiza D, Anaya M, Gómez J, et al. Electronic Tongues and Noses: A General Overview. *Biosensors* 2024;14:190.
66. Santonico M, Pennazza G, Grasso S, et al. Design and test of a biosensor-based multisensorial system: a proof of concept study. *Sensors (Basel)* 2013;13:16625-16640.
67. Persaud K, Dodd G. Analysis of discrimination mechanisms in the mammalian olfactory system using a model nose. *Nature* 1982;299:352-355.
68. Toko K. Taste sensor with global selectivity. *Materials Science and Engineering: C* 1996;4:69-82.
69. Pennazza G, Santonico M, Vollero L, et al. Advances in the Electronics for Cyclic Voltammetry: the Case of Gas Detection by Using Microfabricated Electrodes. *Front Chem* 2018;6:327.

70. Yang H-Y, Chen W-C, Tsai R-C. Accuracy of the Electronic Nose Breath Tests in Clinical Application: A Systematic Review and Meta-Analysis. *Biosensors* 2021;11:469.
71. Sinha R, Lockman KA, Homer NZM, et al. Volatonic analysis identifies compounds that can stratify non-alcoholic fatty liver disease. *JHEP Reports* 2020;2:100137.
72. Verdam FJ, Dallinga JW, Driessen A, et al. Non-alcoholic steatohepatitis: A non-invasive diagnosis by analysis of exhaled breath. *Journal of Hepatology* 2013;58:543-548.
73. Sinha R, Gillespie SL, Brinkman P, et al. Volatomics for Diagnosis and Risk Stratification of MASLD : A Proof-Of-Concept Study. *Aliment Pharmacol Ther* 2025;62:180-192.
74. De Vincentis A, Pennazza G, Santonico M, et al. Breath-print analysis by e-nose for classifying and monitoring chronic liver disease: a proof-of-concept study. *Sci Rep* 2016;6:25337.
75. De Vincentis A, Pennazza G, Santonico M, et al. Breath-print analysis by e-nose may refine risk stratification for adverse outcomes in cirrhotic patients. *Liver International* 2017;37:242-250.
76. Vincentis AD, Vespasiani-Gentilucci U, Sabatini A, et al. Exhaled breath analysis in hepatology: State-of-the-art and perspectives. *WJG* 2019;25:4043-4050.
77. Voss A, Schroeder R, Schulz S, et al. Detection of Liver Dysfunction Using a Wearable Electronic Nose System Based on Semiconductor Metal Oxide Sensors. *Biosensors* 2022;12:70.
78. Sudlow C, Gallacher J, Allen N, et al. UK Biobank: An Open Access Resource for Identifying the Causes of a Wide Range of Complex Diseases of Middle and Old Age. *PLoS Med* 2015;12:e1001779.
79. Dennis A, Kelly MD, Fernandes C, et al. Correlations Between MRI Biomarkers PDFF and cT1 With Histopathological Features of Non-Alcoholic Steatohepatitis. *Front Endocrinol* 2021;11:575843.

Acknowledgments

I would like to express my sincere gratitude to Professor Antonelli Incalzi for his support throughout my doctoral journey.

My heartfelt thanks go to Professor Antonio Picardi, who welcomed me into his group with understanding and affection, making me feel at home.

To Umberto, my tutor, my mentor and guiding light. To Paolo, my other professional half, and my accomplice. They are my strength.

To my colleagues Antonio, Andrea, Valentina, Jessica, Alessandro, Giovanni, and all those who will choose to share part of their journey with us. To my little Giulia.

To all the residents and students who have enriched me, and whom I hope to have enriched in return.

To all my friends, near and far, who have been part of my story.

To my family.

To my parents, without whose unwavering support I could never have become the person I am today.

To my siblings, Caterina and Lorenzo, who are the deepest roots of who I am, and the pieces that make me whole.

To my grandmother, who has always believed in me. To my grandfather, whose memory is a constant source of inspiration.

To my aunt Ofelia, a sweet and precious presence in our family life.

To Sveva, who lights up my heart.